

General Value Function Networks

Matthew Schlegel
 Andrew Jacobsen
 Muhammad Zaheer
 Andrew Patterson
 Adam White
 Martha White

MKSchleg@ualberta.ca
 AJJacobs@ualberta.ca
 MZaheer@ualberta.ca
 AP3@ualberta.ca
 AMW8@ualberta.ca
 WhiteM@ualberta.ca

*Department of Computing Science
 University of Alberta*

Abstract

State construction is important for learning in partially observable environments. A common strategy for state construction is to learn the state update using a Recurrent Neural Network (RNN), which updates the internal state using the current internal state and the most recent observation. This internal state provides a summary of the observed sequence, to facilitate accurate predictions and decision-making. To train RNNs, it is common to approximate gradients back in time, typically with Back-prop Through Time (BPTT). This approximation, however, is sensitive to the truncation window, particularly for environments with long dependencies back-in-time. In this work, we revisit the idea of using predictions to construct state. We formulate an RNN architecture, called a General Value Function Network (GVFN), where each internal state component corresponds to a prediction about the future represented as a value function. We first provide an objective for optimizing GVFNs, and derive several algorithms to optimize this objective. We then show that GVFNs are significantly more robust to train, particularly in terms of the truncation level, in many cases only requiring one-step gradient updates. This work provides a modern re-investigation of the predictive representation hypothesis, and provides evidence that constraining the state to be predictions is promising and merits further investigation.

1. Introduction

Most domains of interest are partially observable, where an agent only observes a limited part of the state. In such a setting, if the agent uses only the immediate observations, it has insufficient information to make accurate predictions or decisions. A natural approach to overcome partial observability is for the agent to maintain a history of interaction. For example, consider an agent in a large and empty room with low-powered sensors that reach only a few meters. In the middle of the room, with just the immediate sensor readings, the agent would not be able to localize itself. Once this limited agent senses a wall, though, it can determine its distance from the wall in the future by remembering this interaction. This simple strategy, however, can be problematic if a long history length is needed [McCallum, 1996].

State construction enables the agent to overcome partial observability, with a more compact representation than an explicit history. Because most environments and datasets are partially observable—in time series prediction, in modelling dynamical systems and in

reinforcement learning—there is a large literature on state construction. These strategies can be separated into Objective-state and Subjective-state approaches.

Objective-state approaches specify a true latent space, and use observations to identify this latent state. Many approaches are designed for a discrete set of latent states, including HMMs [Baum and Petrie, 1966] and POMDPs [Kaelbling et al., 1998]. A classical example is Simultaneous Localization and Mapping, where the agent attempts to extract its position as a part of the state [Durrant-Whyte and Bailey, 2006]. These methods are particularly useful in applications where the dynamics are well-understood or provided, and so accurate transitions can be used in the explicit models. When models need to be estimated or the latent space is unknown, however, these methods either cannot be applied or can be prone to misspecification.

Subjective-state approaches, on the other hand, aim to build an internal state that is a sufficient summary of the past interaction, to make predictions about specific future outcomes. This contrasts objective-state approaches in two key ways. First, the agent is not provided with a true latent space to identify. Second, the agent need not identify a true underlying state, even if there is one; rather, it only needs to identify an internal state that is sufficient for making predictions about the target variables of interest. Such a state could be much simpler than the true underlying state. As such, subjective-state approaches are a more promising direction for online learning agents. Examples of subjective-state approaches to state construction include Recurrent Neural Networks (RNNs) [Hopfield, 1982, Lin and Mitchell, 1993], Predictive State Representations (PSRs) [Littman et al., 2001] and TD Networks [Sutton and Tanner, 2004].

RNNs are a promising subjective-state approach for online state construction, because they are efficient for state updating and simple to use. An RNN provides a recurrent state-update function, where the state is updated as a function of the (learned) state on the previous step and the current observations. These recurrent connections can be unrolled back in time, making it possible for the current RNN state to be dependent on observations far back in time. There have been several specialized activation units crafted to improve learning long-term dependencies, including long short term memory units (LSTMs) [Hochreiter and Schmidhuber, 1997] and gated recurrent units (GRUs) [Cho et al., 2014]. PSRs and TD Networks have not enjoyed the same level of adoption, mainly due to complex algorithms to train these approaches (see [McCracken and Bowling, 2005, Boots et al., 2011] and [Vigorito, 2009, Silver, 2012] respectively). In fact, recent work has investigated facilitating use of these models by combining them with RNNs [Downey et al., 2017, Choromanski et al., 2018, Venkatraman et al., 2017]. Other subjective state approaches based on filtering are typically complicated to extend to nonlinear dynamics, such as system identification approaches [Ljung, 2010] or Predictive Linear Gaussian models [Rudary et al., 2005, Wingate and Singh, 2006].

One issue with RNNs, however, is that training can be unstable and it can be expensive due to computing gradients back-in-time. Real Time Recurrent Learning (RTRL) [Williams and Zipser, 1989] is a real-time algorithm, but is prohibitively expensive: quartic in the hidden dimension size n . Back propagation through time (BPTT) requires maintaining the entire trajectory, which is infeasible for many online learning systems we consider here. A truncated form of BPTT (p-BPTT) is often used to reduce the complexity of training, where complexity grows linearly with p : $O(pn^2)$. Unfortunately, training can be highly sensitive to

the truncation parameters [Pascanu et al., 2013], particularly if the dependencies back-in-time are longer than the chosen p —as we reaffirm in our experiments.

In this paper, we propose a new RNN architecture that is significantly more robust to train. The idea is to constrain the hidden state to be multi-step predictions, using an explicit loss function on the hidden state. In particular, we use general policy-contingent multi-step predictions—called General Value Functions (GVFs) [Sutton et al., 2011]—generalizing the types of predictions considered in related predictive representation architectures [Rafols et al., 2005, Silver, 2012, Sun et al., 2016, Downey et al., 2017]. These GVFs have been shown to represent a wide array of multi-step predictions [Modayil et al., 2014]. We demonstrate through a series of experiments that GVF Networks are effective for representing the state and are much more robust to train, allowing even simple gradient updates with no gradients needed back-in-time. We highlight these properties in three partially observable domains, with long-term dependencies, designed to investigate learning state-update functions in a continual learning setting. We additionally investigate accuracy on two time series datasets, and find that our approach is competitive with a baseline RNN and more robust to BPTT truncation length.

Our work provides additional evidence for the *predictive representation hypothesis*, that state-components restricted to be predictions about the future result in better generalization [Rafols et al., 2005]. Constraining the state to be predictions could both regularize learning—by reducing the hypothesis space for state construction—and prevent the constructed state from overfitting to the observed data and target predictions. To date, there has only been limited investigation into and evidence for this hypothesis. Rafols et al. [2005] showed that, for a discrete state setting, learning was more sample efficient with a predictive representation than a tabular state representation and a tabular history representation. Schaul and Ring [2013] showed how a collection of optimal GVFs—learned offline—provide a better state representation for a reward maximizing task, than a collection of optimal PSR predictions. Sun et al. [2016] showed that, for dynamical systems, constraining state to be predictions about the future significantly improved convergence rates over auto-regressive models and n4sid. There has also been some evidence for a related idea: using predictions as auxiliary tasks to promote generalization. This approach does not change the RNN architecture—nor explicitly use the predictive representation hypothesis—because these predictions are simply added to the set of targets. There seem to be some benefits in reinforcement learning from this addition, such as in the Unreal architecture [Jaderberg et al., 2016], and for modelling dynamical systems, such as in Predictive State Decoders [Venkatraman et al., 2017]. We provide a preliminary comparison to this alternative idea, to better investigate the utility of explicitly using predictions as state. Our experiments show that predictive state components have a distinct advantage over RNNs augmented with auxiliary tasks, providing more evidence for the predictive representation hypothesis.

2. Problem Formulation

We consider a partially observable setting, where the observations are a function of an unknown, unobserved underlying state. The dynamics are specified by transition probabilities $P = \mathcal{S} \times \mathcal{A} \times \mathcal{S} \rightarrow [0, \infty)$ with state space \mathcal{S} and action-space \mathcal{A} . On each time step the agent receives an observation vector $\mathbf{o}_t \in \mathcal{O} \subset \mathbb{R}^m$, as a function $\mathbf{o}_t = \mathbf{o}(z_t)$ of the underlying

state $z_t \in \mathcal{S}$. The agent only observes \mathbf{o}_t , not z_t , and then takes an action a_t , producing a sequence of observations and actions: $a_0, \mathbf{o}_1, a_1, \dots$

The goal for the agent under partial observability is to identify a state representation $\mathbf{s}_t \in \mathbb{R}^n$ which is a sufficient statistic (summary) of past interaction. More precisely, such a *sufficient states* would ensure that predictions y_t about future outcomes given this state are independent of history $\mathbf{h}_t = a_0, \mathbf{o}_1 \dots, a_{t-1}, \mathbf{o}_t$, i.e. for any $i > 0$

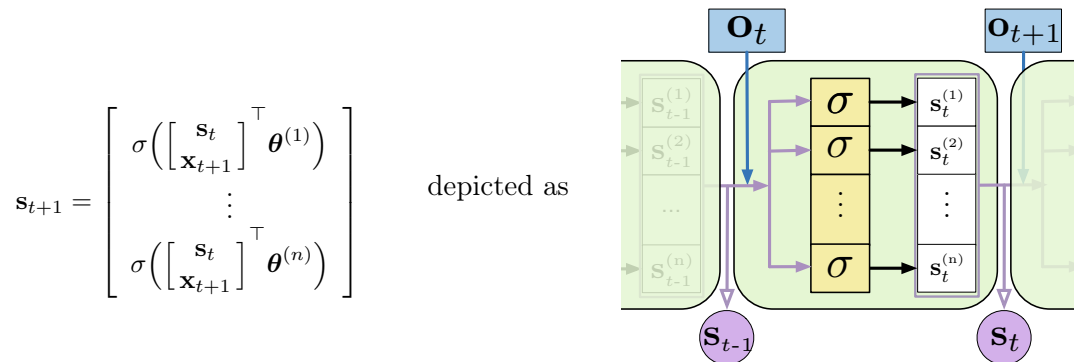
$$p(y_{t+i}|\mathbf{s}_t) = p(y_{t+i}|\mathbf{s}_t, \mathbf{h}_t). \quad (1)$$

Such a state summarizes the history, removing the need to store the entire (potentially infinite) history.

One strategy for learning a state is with *recurrent neural networks* (RNNs), which learn a state-update function. Imagine a setting where the agent has a sufficient state \mathbf{s}_t for this step. To obtain sufficient state for the next step, it simply needs to update \mathbf{s}_t with the new information in the given observation and action $\mathbf{x}_{t+1} = [\mathbf{o}_{t+1}, a_t, a_{t+1}] \in \mathbb{R}^d$. The goal, therefore, is to learn a state-update function $f : \mathbb{R}^{n+d} \rightarrow \mathbb{R}^n$ such that

$$\mathbf{s}_{t+1} = f(\mathbf{s}_t, \mathbf{x}_{t+1}) \quad (2)$$

provides a sufficient state \mathbf{s}_{t+1} . The update function f is parameterized by a weight vector $\boldsymbol{\theta} \in \Theta$ in some parameter space Θ . An example of a simple RNN update function, for $\boldsymbol{\theta}$ composed of stacked vectors $\boldsymbol{\theta}^{(j)} \in \mathbb{R}^{n+d}$ for each hidden state $j \in \{1, \dots, n\}$ is, for activation function $\sigma : \mathbb{R} \rightarrow \mathbb{R}$,



The goal in this work is to develop an efficient algorithm to learn this state-update function, particularly one that is not dependent on number of steps back-in-time. Most RNN algorithms learn this state-update by minimizing prediction error to desired targets $y_t \in \mathbb{R}$ across time. For example, for $\hat{y}_t = \mathbf{s}_t^\top \mathbf{w}$ for weights $\mathbf{w} \in \mathbb{R}^n$, the loss for $\boldsymbol{\theta}$ on time step t could be

$$\begin{aligned} \ell(\hat{y}_t, y_t) &\stackrel{\text{def}}{=} (\hat{y}_t - y_t)^2 \\ &= (\mathbf{s}_t^\top \mathbf{w} - y_t)^2 \\ &= (f_{\boldsymbol{\theta}}(\mathbf{s}_{t-1}, \mathbf{x}_t)^\top \mathbf{w} - y_t)^2 = \left(f_{\boldsymbol{\theta}}\left(f_{\boldsymbol{\theta}}(\mathbf{s}_{t-2}, \mathbf{x}_{t-1}), \mathbf{x}_t\right)^\top \mathbf{w} - y_t\right)^2 = \dots \end{aligned}$$

We pursue an alternative strategy, inspired by predictive representations, where the state-update function is learned such that each hidden state is an accurate prediction about future outcomes.

3. Constraining State to be Predictions

Let us start in a simpler setting and explain how the hidden units could be trained to be n -horizon predictions about the future. Imagine you have a multi-dimensional time series of a power-plant, consisting of d sensory observations with the first sensory corresponding to water temperature. Your goal is to make a hidden node in your RNN predict the water temperature in 10 steps, because you think this feature is useful to make other predictions about the future.

This can be done simply by adding the following loss: $(\mathbf{s}_{t,1} - \mathbf{x}_{t+10,1})^2$. The combined loss $L_t(\boldsymbol{\theta})$ on time step t is

$$L_t(\boldsymbol{\theta}) \stackrel{\text{def}}{=} \ell(\hat{y}_t, y_t) + (\mathbf{s}_{t,1} - \mathbf{x}_{t+10,1})^2 \quad (3)$$

where both \hat{y}_t and \mathbf{s}_t are implicitly functions of $\boldsymbol{\theta}$. This loss still encourages the RNN to find a hidden state \mathbf{s}_t that predicts y_t well. There is likely a whole space of solutions that have similar accuracy for this prediction. The second loss constrains this search to pick a solution where the first state node is a prediction about an observation 10 steps into the future. This second term can be seen as a regularizer on the network, specifying a preference on the learned solution. In general, more than one state node—even all of \mathbf{s}_t —could be learned to be predictions about the future.

The difficulty in training such a state depends on the chosen targets. For example, long horizon targets—such as 100 steps rather than 10 steps into the future—can be high variance. Even if such a predictive feature could be useful, it may be difficult to learn accurately and could make the state-update less stable. Using n -horizon predictions also requires a delay in the update: the agent must wait 100 steps to see the target to update the state at time t .

We therefore propose to restrict ourselves to a class of prediction that have been shown to be more robust to these issues [van Hasselt and Sutton, 2015, Sutton et al., 2011, Modayil et al., 2014]. This class of predictions correspond to predictions of discounted cumulative sums of signals into the future, called General Value Functions (GVFs). We have algorithms to estimate these predictions online, without having to wait to see outcomes in the future. We believe the ability to update online is critical for RNNs, which are typically deployed in an online setting. Further, it is possible that this class of predictions is sufficient, and so the restricting to GVFs does not significantly limit representability. We therefore focus on developing an approach for this class of predictions within RNNs.

4. GVF Networks

In this section, we introduce GVF Networks, an RNN architecture where hidden states are constrained to predict policy-contingent, multi-step outcomes about the future. We first describe GVFs and the GVF Network (GVFN) architecture. In the following section, we develop the objective function and algorithm to learn GVFNs. There are several related predictive approaches, in particular TD Networks, that we discuss in Section 8, after introducing GVFNs.

We first need to extend the definition of GVFs [Sutton et al., 2011] to the partially observable setting, to use them within RNNs. The first step is to replace state with histories. We define \mathcal{H} to be the minimal set of histories, that enables the Markov property for the

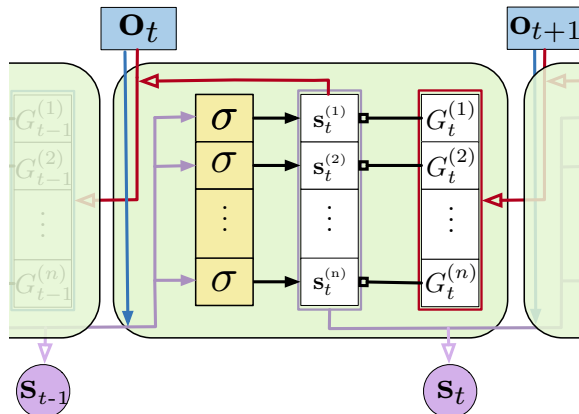


Figure 1: GVF Networks (GVFNs), where each state component $s_t^{(i)}$ is updated towards the return $G_t^{(i)} \stackrel{\text{def}}{=} C_{t+1}^{(i)} + \gamma_{t+1}^{(i)} s_{t+1}^{(i)}$ for the i th GVF; this learning target is indicated by the connections with squares. The observation and state on the next step is used to define the target on this step, indicate by the blue arrows.

distribution over next observation

$$\mathcal{H} = \left\{ \mathbf{h}_t = (a_0, \mathbf{o}_1, \dots, a_{t-1}, \mathbf{o}_t) \mid \begin{array}{l} \text{(Markov property)} \Pr(\mathbf{o}_{t+1} | \mathbf{h}_t, a_t) = \Pr(\mathbf{o}_{t+1} | a_{-1}, \mathbf{o}_{-1}, \mathbf{h}_t, a_t), \\ \text{(Minimal history)} \Pr(\mathbf{o}_{t+1} | \mathbf{h}_t) \neq \Pr(\mathbf{o}_{t+1} | a_1, \mathbf{o}_2, \dots, a_{t-1}, \mathbf{o}_t) \end{array} \right\} \quad (4)$$

A GVF question is a tuple (π, c, γ) composed of a policy $\pi : \mathcal{H} \times \mathcal{A} \rightarrow [0, \infty)$, cumulant $c : \mathcal{H} \rightarrow \mathbb{R}$ and continuation function $\gamma : \mathcal{H} \rightarrow [0, 1]$. The answer to a GVF question is defined as the value function, $V : \mathcal{H} \rightarrow \mathbb{R}$, which gives the expected, cumulative discounted cumulant from any history $\mathbf{h}_t \in \mathcal{H}$, which can be defined recursively with a Bellman equation as

$$\begin{aligned} V(\mathbf{h}_t) &\stackrel{\text{def}}{=} \mathbb{E}[c(H_{t+1}) + \gamma(H_{t+1})V(H_{t+1}) \mid H_t = \mathbf{h}_t, A_t \sim \pi(\cdot | \mathbf{h}_t)] \\ &= \sum_{a_t \in \mathcal{A}} \pi(a_t | \mathbf{h}_t) \sum_{\mathbf{h}_{t+1} \in \mathcal{H}} \Pr(\mathbf{h}_{t+1} | \mathbf{h}_t, a_t) [c(\mathbf{h}_{t+1}) + \gamma(\mathbf{h}_{t+1})V(\mathbf{h}_{t+1})]. \end{aligned} \quad (5)$$

The sums can be replaced with integrals if \mathcal{A} or \mathcal{O} are continuous sets.

A GVFN is an RNN, and so is a state-update function f , but with the additional criteria that each element in \mathbf{s}_t corresponds to a prediction—to a GVF. A GVFN is composed of n GVFs, with each hidden state component \mathbf{s}_j trained such that at time step t , $\mathbf{s}_j \approx V^{(j)}(\mathbf{h}_t)$ for the j th GVF and history \mathbf{h}_t . Each hidden state component, therefore, is a prediction about a multi-step policy-contingent question. The hidden state is updated recurrently as $\mathbf{s}_t \stackrel{\text{def}}{=} f_{\theta}(\mathbf{s}_{t-1}, \mathbf{x}_t)$ for a parametrized function f_{θ} , where $\mathbf{x}_t = [\mathbf{o}_t, a_t]$ and f_{θ} is trained so that $\mathbf{s}_j \approx V^{(j)}(\mathbf{h}_t)$. This is summarized in Figure 1.

General value functions provide a rich language for encoding predictive knowledge. In their simplest form, GVFs with constant γ correspond to multi-timescale predictions referred to as Nexting predictions [Modayil et al., 2014]. Allowing γ to change as a function of state or history, GVF predictions can combine finite-horizon prediction with predictions that terminate when specific outcomes are observed [Modayil et al., 2014].

To build some intuition, we provide some examples in Compass World. This environment is used in our experiments and depicted in Figure 2. Compass World is a grid world where

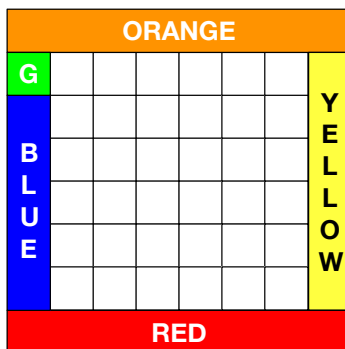


Figure 2: The Compass World: A partially observable grid world with observations of the color directly in front of the agent. **Observations:** The agent will observe the color of the grid cell it is facing. This means the agent can only observe a colored wall at the edge of the environment facing outward. **Actions:** The agent can take the forward, left, and right actions. **Goal:** The agent’s goal is to make accurate predictions about which direction it is facing. These predictions can be encoded as GVFs.

the agent is only provided information about the color directly in front it. This world is partially observable, with all the tiles in the middle having a white observation, with the only distinguishing color information available to the agent at the walls. The actions taken by the agent are to move forward, turn left, or turn right.

In this environment, the agent might want to know if it is facing the red wall. This can be specified as a GVF question: “If I go forward until I hit a wall, what is the probability I will see red?”. The policy is to always go forward. If the agent hits a wall—it sees a color—then γ is zero, terminating the sum of cumulants to that point. If the current observation is ‘Red’, then the cumulant is 1; otherwise it is zero. The sampled return from a state is 1.0 if the agent is facing the Red wall, because going forward will result in summing many zero plus a 1 right before termination. If the agent is not facing the Red wall, the return is 0, because the agent terminates when hitting the wall but only sees cumulants that are zero for the entire trajectory. Because the outcome is deterministic, the probabilities are 1 or 0.

The agent could also ask the probability of seeing Red within a horizon of about 10 steps. In this case, the continuation would be 0.9 until seeing ‘Red’. The intuition for this comes from thinking of $1 - \gamma$ as a success probability for a geometric distribution: the probability of successfully terminating. The mean of this geometric distribution is $\frac{1}{1-\gamma}$, which in this case is $\frac{1}{1-0.9} = 10$. With constant γ , the prediction corresponds to the amount an observation is seen within that time horizon. For example, for a constant γ of 0.99, with a cumulant of 1 when seeing ‘Red’ and zero otherwise and a random policy, the GVF question is “How frequently will I see ‘Red’ within the next 100 steps, if I drive around randomly?”.

Notice that though we define the cumulants and continuation functions on the underlying (unknown) state \mathbf{h}_t , this is a generalization of defining it on the observations. The observations are a function of state; the cumulants and continuations γ that are defined on observations are therefore defined on \mathbf{h}_t . In the examples above, these functions were defined using just the observations. More generally, we consider them as part of a problem definition. This means they could be defined using short histories, or other separate summaries of the history.

As we discuss in Section 6, we can also consider cumulants that are a function of our own predictions or constructed state.

A natural question is how these GVFs are chosen. This problem corresponds to the discovery problem for predictive representations. In this work, we first focus on the utility of this architecture, with simple heuristics or expert chosen GVFs. We leave a more systematic investigation of the discovery problem to future work.

5. A Case Study using GVFNs for Time Series Prediction

Before discussing the objective and training algorithms for GVFNs, we provide a simple demonstration of their use in a synthetic single-variable time series dataset, to build intuition. GVFNs can be used for time series prediction, simply by assuming that a fixed (unknown) policy generates the data. The GVFs within the network all have the same policy, with different continuation functions γ and potentially different cumulants. For example, for a multi-variate time series, one GVF could have a cumulant corresponding to the first entry of the observation on the next time step, and another GVF could use the second entry. Even for a single-variate time series, GVFs can have different cumulants. For example, one GVF could correspond to the probability that the observation becomes larger than 1. Then the cumulant would be zero until this event occurs, at which point it would be 1. In our experiment, we use one of the simplest choices: the GVFs all have the same cumulant and policy, with different constants γ .

In this experiment, we use the single-variate Mackey-Glass time series dataset, which is synthesized from a time-delay differential equation.

$$\frac{\partial y(t)}{\partial t} = \alpha \frac{y(t - \tau)}{1 + y(t - \tau)^{10}} - \beta y(t). \quad (6)$$

We follow the learning setup in Bianchi et al. [2017]. We use $\tau = 17$, $\alpha = 0.2$, and $\beta = 0.1$. We take integration steps of size 0.1. We forecast the target variable y twelve steps into the future, starting from an initial value $y(0) = 1.2$.

We used 128 GVFs with γ 's selected linearly in the range $[0.1, 0.97]$. The GVFN is trained using semi-gradient TD(0), described in more detail in Section 7. The architecture for the GVFN uses a linear layer for the state update and a ReLU layer to predict the targets:

$$\mathbf{s}_{t+1} = \begin{bmatrix} \begin{bmatrix} \mathbf{s}_t \\ \mathbf{o}_{t+1} \end{bmatrix}^\top \boldsymbol{\theta}^{(1)} \\ \vdots \\ \begin{bmatrix} \mathbf{s}_t \\ \mathbf{o}_{t+1} \end{bmatrix}^\top \boldsymbol{\theta}^{(n)} \end{bmatrix} \quad \hat{y}_{t+12} = \max(0, \mathbf{s}_t \mathbf{W}) \boldsymbol{\beta}$$

where $\mathbf{W} \in \mathbb{R}^{128 \times 32}$ and $\boldsymbol{\beta} \in \mathbb{R}^{32}$. We included a baseline RNN trained using BPTT with a truncation lengths of $\rho \in \{1, 2, 4, 8, 16, 32\}$ steps and an Adam optimizer. The RNN had the equivalent architecture to the GVFN: a hidden layer of 32 units followed by a linear output layer. The goal of this experiment is just to show how GVFNs can be used in problems where RNNs can be used; our goal is not necessarily to outperform the RNN.

Figure 3 shows the learning curves for this experiment. The main result is that the simplest GVFN algorithm, simple one-step TD updates with *no* BPTT, can obtain high

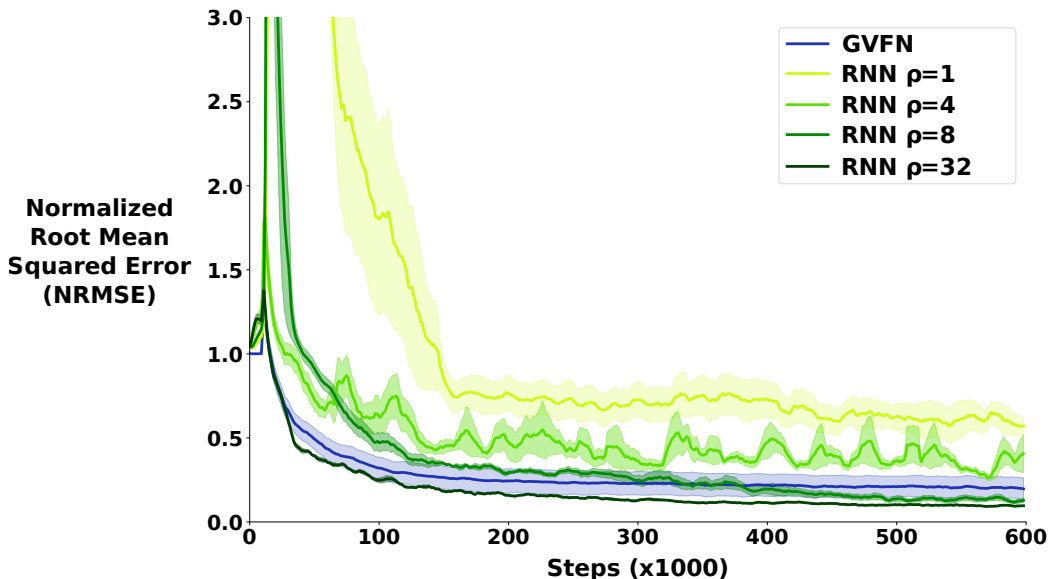


Figure 3: Learning curves (NRMSE) for a linear GVFN and baseline RNN on the Mackey-Glass dataset. The GVFN is learned using semi-gradient TD with linear value function approximation. The RNN is trained using BPTT with various truncation lengths.

accuracy on this dataset. The GVFs within the GVFN were not specially designed for this time series problem, and so there is some promise for this being a sufficiently general RNN network architecture. The GVFN is competitive with the RNN baseline, performing at least as well for all $\rho < 32$.

6. The Objective for GVFNs

In this section, we introduce the objective function for GVFNs, that constrains the learned state to be GVF predictions. Each state component of a GVFN is a value function prediction, and so is approximating the fixed point to a Bellman equation with history in Equation (5). The extension is not as simple as using a standard Bellman operator, however, because the GVFs are in a network. In fact, the Bellman equations are coupled in two ways: through composition—where one GVF can be the cumulant for another GVF—and through the parametric recurrent state representation. We first consider the Bellman Network operator in Section 6.1, which extends the typical Bellman operator to allow for composition. We then explain how the coupling that arises from the recurrent state representation can be handled using a projected operator, and provide the objective for GVFNs, called the Mean-Squared Projected Bellman Network Error (MSPBNE), in Section 6.2. Then we discuss several algorithms to optimize this objective in Section 7.

Note that this objective can be used in addition to the standard RNN objective, which optimizes state to improve predictions for a given target. The GVFN objective we introduce can be added to the standard RNN objective, to provide an RNN where the learned states are both useful for prediction of the target and encouraged—or regularized—to be GVF predictions. In this work, we only train GVFNs with the GVFN objective, without including

the loss to a target, to focus the investigation on the utility of the proposed objective and on predictive features.

6.1 The Bellman Network Operator

To understand the Bellman Network operator, it is useful to first revisit the Bellman operator for learning a single GVF. Assume the values are encoded as a table, $\mathbf{V}^{(j)} \in \mathbb{R}^{|\mathcal{H}|}$, for a GVF question $(\pi^{(j)}, c^{(j)}, \gamma^{(j)})$. The Bellman equation in 5 can be written as a fixed point equation, with Bellman operator

$$\mathbf{B}^{(j)}\mathbf{V}^{(j)} \stackrel{\text{def}}{=} \mathbf{C}^{(j)} + \mathbf{P}^{(j)}\mathbf{V}^{(j)} \quad (7)$$

where $\mathbf{C}^{(j)} \in \mathbb{R}^{|\mathcal{H}|}$ is the vector of expected cumulant values under $\pi^{(j)}$, with entries

$$\mathbf{C}^{(j)}(\mathbf{h}_t) \stackrel{\text{def}}{=} \sum_{a_t \in \mathcal{A}} \pi^{(j)}(a_t | \mathbf{h}_t) \sum_{\mathbf{h}_{t+1} \in \mathcal{H}} \text{Pr}(\mathbf{h}_{t+1} | \mathbf{h}_t, a_t) c^{(j)}(\mathbf{h}_{t+1}). \quad (8)$$

and $\mathbf{P}^{(j)} \in \mathbb{R}^{|\mathcal{H}| \times |\mathcal{H}|}$ is the matrix of values satisfying

$$\mathbf{P}^{(j)}(\mathbf{h}_t, \mathbf{h}_{t+1}) = \sum_{a_t \in \mathcal{A}} \pi^{(j)}(a_t | \mathbf{h}_t) \text{Pr}(\mathbf{h}_{t+1} | \mathbf{h}_t, a_t) \gamma^{(j)}(\mathbf{h}_{t+1}). \quad (9)$$

If the operator $\mathbf{B}^{(j)}$ is a contraction, then iteratively applying this operator converges to a fixed point. More precisely, if for any $\mathbf{V}_1^{(j)}, \mathbf{V}_2^{(j)} \in \mathbb{R}^{|\mathcal{H}|}$, $\|\mathbf{B}^{(j)}\mathbf{V}_1^{(j)} - \mathbf{B}^{(j)}\mathbf{V}_2^{(j)}\| < \|\mathbf{V}_1^{(j)} - \mathbf{V}_2^{(j)}\|$, then iteratively applying $\mathbf{B}^{(j)}$, as $\mathbf{V}_2^{(j)} = \mathbf{B}^{(j)}\mathbf{V}_1^{(j)}, \dots, \mathbf{V}_{t+1}^{(j)} = \mathbf{B}^{(j)}\mathbf{V}_t^{(j)}, \dots$, converges to a fixed point. Because temporal difference learning algorithms are based on this fixed-point update, the Bellman operator is central to the analysis of many algorithms for learning value functions, and is used in the definition of objectives for value estimation.

We can similarly define a Bellman operator that accounts for the relationships between GVFs in the network. Assume there are n GVFs, with $\mathbf{V} \in \mathbb{R}^{n|\mathcal{H}|}$ the stacked values for all the GVFs,

$$\mathbf{V} \stackrel{\text{def}}{=} \begin{bmatrix} \mathbf{V}^{(1)} \\ \vdots \\ \mathbf{V}^{(n)} \end{bmatrix}. \quad (10)$$

The cumulants may now be functions of the values of other GVFs; we therefore explicitly write $\mathbf{C}_{\mathbf{V}}^{(j)}$. The Bellman Network operator \mathbf{B} is

$$\mathbf{B}\mathbf{V} \stackrel{\text{def}}{=} \begin{bmatrix} \mathbf{C}_{\mathbf{V}}^{(1)} + \mathbf{P}^{(1)}\mathbf{V}^{(1)} \\ \vdots \\ \mathbf{C}_{\mathbf{V}}^{(n)} + \mathbf{P}^{(n)}\mathbf{V}^{(n)} \end{bmatrix}. \quad (11)$$

The Bellman Network operator needs to be treated as a joint operator on all the GVFs because of compositional predictions, where the prediction on the next step of GVF j is the cumulant for GVF i . When iterating the Bellman operator $\mathbf{V}^{(j)}$ is not only involved in its own Bellman equation, but also in the Bellman equation for $\mathbf{V}^{(i)}$. Notice that if there were no compositions, the Bellman Network operator would separate into individual Bellman operators, that operate on each $\mathbf{V}^{(j)}$ independently.

To use such a Bellman Network operator, we need to ensure that iterating under this operator converges to a fixed point. For no composition, this result is straightforward, as it simply follows from previous results showing when the Bellman operator is a contraction. We state this explicitly below in Corollary 1. Under composition, we need to consider the effect of the current value function on the cumulant. Consequently, the operator may no longer be a simple linear projection of the values, followed by a sum of expected cumulants.

We first identify a necessary condition: the connections between GVFs be acyclic. For example, GVF i cannot be a cumulant for GVF j , if j is already a cumulant for i . More generally, the connections between GVFs cannot create a cycle, such as $1 \rightarrow 2 \rightarrow 3 \rightarrow 1$. We provide a counterexample, where the Bellman Network operator is not a contraction when there is a cycle, to illustrate that this condition is necessary.

We further place restrictions on the cumulant, as a function of other GVFs. In particular, we require that the cumulant is a linear function of the values of other GVFs. Note that this restriction encompasses the setting for a non-compositional GVF, because the cumulant can be a constant w.r.t. these values. This linearity condition is unlikely to be necessary, but does significantly simplify the proof. Further, in all our experiments, we only use linear functions of values, and so restrict attention to that case for now.

Assumption 1 (Acyclic Connections). *The directed graph G is acyclic. G consists of n vertices, each corresponding to a GVF, and each directed edge (i, j) indicates that j is used in the cumulant for i .*

Assumption 2 (Linear Composition). *If GVF i has directed edges to $\{j_1, \dots, j_k\}$, then for some weights $w_1, \dots, w_k \in \mathbb{R}$, the cumulant must satisfy $c_{j, \mathbf{V}}(\mathbf{h}_{t+1}) = \sum_{l=1}^k w_l \mathbf{V}^{(j_l)}(\mathbf{h}_{t+1})$ or equivalently, $\mathbf{C}_{\mathbf{V}}^{(i)} = \sum_{l=1}^k w_l \mathbf{P}^{(j_l)} \mathbf{V}^{(j_l)}$.*

Assumption 3 (Discounted Transitions are Contractions). *For all $j \in \{1, \dots, n\}$, $\beta_j \stackrel{\text{def}}{=} \|\mathbf{P}^{(j)}\| < 1$.*

With these three assumptions, we can prove the main result. The third assumption is standard for showing Bellman operators are contractions, and is easily satisfied if the policy is proper: is guaranteed to visit a state where the discount is less than 1. The second assumption assumes that a compositional GVF uses values directly on the next step. In the simplest setting, where the cumulant for GVF i is the value of GVF j on the next step, then there is only one edge (i, j) and $c_{j, \mathbf{V}}(\mathbf{h}_{t+1}) = \mathbf{V}^{(j)}(\mathbf{h}_{t+1})$ or equivalently, $\mathbf{C}^{(i)} = \mathbf{P}^{(j)} \mathbf{V}^{(j)}$. More general linear settings could be considered, such as values two or more steps into the future, with a similar proof.

Theorem 1. *Under Assumptions 1-3, iterating $\mathbf{V}_{t+1} = \mathbf{B}\mathbf{V}_t$ converges to a unique fixed point.*

Proof. We cannot rely on the Bellman network operator being a contraction on each step. Rather, we explicitly prove that the sequence converges (Part 1) and that it converges to a unique fixed point (Part 2 and 3).

Part 1: *The sequence $\mathbf{V}_1, \mathbf{V}_2, \dots$ defined by $\mathbf{V}_{t+1} = \mathbf{B}\mathbf{V}_t$ converges to a limit $\mathbf{V}^* \in \mathbb{R}^{n|\mathcal{H}|}$.*

Because G is acyclic, we have a linear topological ordering of the vertices, i_1, \dots, i_n , where for each directed edge (i, j) , i comes before j in the ordering. Therefore, starting from

the last GVF j , we know that the Bellman operator $\mathbf{B}^{(j)}$ is a contraction with rate $\beta_j < 1$,

$$\|\mathbf{B}^{(j)}\mathbf{V}_1^{(j)} - \mathbf{B}^{(j)}\mathbf{V}_0^{(j)}\| = \|\mathbf{P}^{(j)}\mathbf{V}_1^{(j)} - \mathbf{P}^{(j)}\mathbf{V}_0^{(j)}\| \leq \beta_j \|\mathbf{V}_1^{(j)} - \mathbf{V}_0^{(j)}\|.$$

Therefore, iterating \mathbf{B} for t steps results in the error

$$\|\mathbf{V}_{t+1}^{(j)} - \mathbf{V}_t^{(j)}\| \leq \beta_j^t \|\mathbf{V}_1^{(j)} - \mathbf{V}_0^{(j)}\|$$

and as $t \rightarrow \infty$, $\mathbf{V}_t^{(j)}$ converges to its fixed point.

We will use induction for the argument, with the above as the base case. Assume for all $j \in \{i_k, \dots, i_n\}$ there exists a ball of radius $\epsilon_j(t)$ where $\|\mathbf{V}_{t+1}^{(j)} - \mathbf{V}_t^{(j)}\| \leq \epsilon_j(t)$ and $\epsilon_j(t) \rightarrow 0$ as $t \rightarrow \infty$. Consider the next GVF in the ordering, $i = i_{k-1}$.

Case 1: there are no outgoing edges from i . If i does not use another GVF j in its cumulant, then iterating with \mathbf{B} independently iterates $\mathbf{V}_t^{(i)}$ with $\mathbf{B}^{(i)}$. Therefore, as above, $\mathbf{V}_t^{(i)}$ converges because the Bellman operator is a contraction. In this setting, clearly such an $\epsilon_i(t)$ exists because $\|\mathbf{V}_{t+1}^{(i)} - \mathbf{V}_t^{(i)}\| \rightarrow 0$ as $t \rightarrow \infty$.

Case 2: Consider the case where the cumulant for i is the value for GVF j on the next step—one outgoing edge (i, j) and weight w_1 set to 1. The update on each step is $\mathbf{V}_{t+1}^{(i)} = \mathbf{P}^{(j)}\mathbf{V}_t^{(j)} + \mathbf{P}^{(i)}(\mathbf{V}_t^{(i)} - \mathbf{V}_{t-1}^{(i)})$. Under the inductive hypothesis, we know that $\|\mathbf{V}_{t+1}^{(j)} - \mathbf{V}_t^{(j)}\| \leq \epsilon_j(t)$ for cumulant j . As a result, the change in $\mathbf{V}_t^{(i)}$ is

$$\begin{aligned} \|\mathbf{V}_{t+1}^{(i)} - \mathbf{V}_t^{(i)}\| &= \|\mathbf{P}^{(j)}(\mathbf{V}_t^{(j)} - \mathbf{V}_{t-1}^{(j)}) + \mathbf{P}^{(i)}(\mathbf{V}_t^{(i)} - \mathbf{V}_{t-1}^{(i)})\| \\ &\leq \|\mathbf{V}_t^{(j)} - \mathbf{V}_{t-1}^{(j)}\| + \beta_i \|\mathbf{V}_t^{(i)} - \mathbf{V}_{t-1}^{(i)}\| \\ &\leq \epsilon_j(t-1) + \beta_i \|\mathbf{V}_t^{(i)} - \mathbf{V}_{t-1}^{(i)}\| \end{aligned}$$

For sufficiently large t , $\epsilon_j(t-1)$ can be made arbitrarily small. If $\epsilon_j(t-1) < (1 - \beta_i)\|\mathbf{V}_t^{(i)} - \mathbf{V}_{t-1}^{(i)}\|$, then

$$\|\mathbf{V}_{t+1}^{(i)} - \mathbf{V}_t^{(i)}\| \leq \tilde{\beta}_i \|\mathbf{V}_t^{(i)} - \mathbf{V}_{t-1}^{(i)}\| \quad \text{for some } \tilde{\beta}_i < 1$$

and so the iteration is a contraction on step t . Else, if $\epsilon_j(t-1) \geq (1 - \beta_i)\|\mathbf{V}_t^{(i)} - \mathbf{V}_{t-1}^{(i)}\|$, then this implies the difference $\|\mathbf{V}_{t+1}^{(i)} - \mathbf{V}_t^{(i)}\|$ is already within a very small ball, with radius $\epsilon_j(t-1)/(1 - \beta_i)$. As $t \rightarrow \infty$, the difference can oscillate between being within this ball, which shrinks to zero, or being iterated with a contraction that also shrinks the difference. In either case, there exists an $\epsilon_i(t)$ such that $\|\mathbf{V}_{t+1}^{(i)} - \mathbf{V}_t^{(i)}\| \leq \epsilon_i(t)$, where $\epsilon_i(t) \rightarrow 0$ as $t \rightarrow \infty$.

Case 3: More generally, GVF i can have a weighted sum of GVFs j_1, \dots, j_k for its cumulant. The argument for this case is similar to the argument for Case 2, simply with a weighted sum of $\epsilon_{j_1}(t), \dots, \epsilon_{j_k}(t)$.

Because we have such an ϵ_i for all GVFs in the network, we know the sequence $\mathbf{V}_t^{(i)}$ converges.

Part 2: \mathbf{V}^* is a fixed point of \mathbf{B} .

Because the Bellman network operator is continuous, the limit can be taken inside the operator

$$\mathbf{V}^* = \lim_{t \rightarrow \infty} \mathbf{V}_t = \lim_{t \rightarrow \infty} \mathbf{B}\mathbf{V}_{t-1} = \mathbf{B}\left(\lim_{t \rightarrow \infty} \mathbf{V}_{t-1}\right) = \mathbf{B}\mathbf{V}^*$$

Part 3: \mathbf{V}^* is the only fixed point of \mathbf{B} .

Consider an alternative solution \mathbf{V} . Because of the uniqueness of fixed points under Bellman operators, all those GVF's that have non-compositional cumulants have unique fixed points and so those components in \mathbf{V} must be the same as \mathbf{V}^* . All the GVF's next in the ordering that use those GVF's as cumulants have a unique cumulant, and so must then also converge to a unique value, because their Bellman operators with fixed GVF's as cumulants have a unique fixed point. This argument continues for the remaining GVF's in the ordering. ■

Corollary 1. *Under Assumption 3 with non-compositional cumulants (no edges in G), iterating $\mathbf{V}_{t+1} = \mathbf{B}\mathbf{V}_t$ converges to a unique fixed point.*

Proposition 1 (Necessity of Acyclic Composition). *There exists transition function $\mathbf{P} : \mathcal{S} \times \mathcal{A} \times \mathcal{S} \rightarrow [0, 1]$ and policy $\pi : \mathcal{S} \times \mathcal{A} \rightarrow [0, 1]$ such that, for two GVF's in a cycle, iteration with the Bellman Network operator diverges.*

Proof. Assume there are two states, with the policy defined such that we get the following dynamics for the Markov chain

$$\mathbf{P}^\pi = \begin{bmatrix} 0.9 & 0.1 \\ 0.1 & 0.9 \end{bmatrix}. \tag{12}$$

Assume further that $\gamma = 0.95$. The resulting Bellman iteration is

$$\begin{aligned} \begin{bmatrix} \mathbf{V}^{(1)} \\ \mathbf{V}^{(2)} \end{bmatrix} &= \mathbf{P}^\pi \begin{bmatrix} \mathbf{V}^{(2)} \\ \mathbf{V}^{(1)} \end{bmatrix} + \gamma \mathbf{P}^\pi \begin{bmatrix} \mathbf{V}^{(1)} \\ \mathbf{V}^{(2)} \end{bmatrix} \\ &= \mathbf{P}^\pi \begin{bmatrix} 0 & 1 \\ 1 & 0 \end{bmatrix} \begin{bmatrix} \mathbf{V}^{(1)} \\ \mathbf{V}^{(2)} \end{bmatrix} + \mathbf{P}^\pi \begin{bmatrix} \gamma & 0 \\ 0 & \gamma \end{bmatrix} \begin{bmatrix} \mathbf{V}^{(1)} \\ \mathbf{V}^{(2)} \end{bmatrix} \\ &= \mathbf{P}^\pi \begin{bmatrix} \gamma & 1 \\ 1 & \gamma \end{bmatrix} \begin{bmatrix} \mathbf{V}^{(1)} \\ \mathbf{V}^{(2)} \end{bmatrix} \end{aligned}$$

Since the matrix $\mathbf{P}^\pi \begin{bmatrix} \gamma & 1 \\ 1 & \gamma \end{bmatrix}$ is an expansion, for many initial $\begin{bmatrix} \mathbf{V}^{(1)} \\ \mathbf{V}^{(2)} \end{bmatrix}$ this iteration goes to infinity, such as initial $\mathbf{V}^{(1)} = \mathbf{V}^{(2)} = \begin{bmatrix} 1 \\ 1 \end{bmatrix}$. ■

6.2 The Objective Function for GVFNs

With a valid Bellman Network operator, we can proceed to defining the objective function for GVFNs. The above fixed point equation assumes a tabular setting, where the values can be estimated directly for each history. GVFNs, however, have a restricted functional form, where the value estimates must be a parametrized function of the current observation and value predictions from the last time step. Under such a functional form, it is unlikely that we can exactly solve for the fixed point.¹ Rather, we will solve for a projected fixed point, which projects into the space of representable value functions.

1. One approach to exactly solve such an equation has been to define a belief state, as in POMDPs, and solve for the value function as a function of belief state. These approaches guarantee that the fixed point can be obtained; however, they also require identification of the belief state with an NP-Hard problem formulation.

Define the space of functions as

$$\mathcal{F} = \left\{ \mathbf{V}_\theta = [\mathbf{V}_\theta^{(1)}, \dots, \mathbf{V}_\theta^{(n)}] \in \mathbb{R}^{n|\mathcal{H}|} \mid \text{where } \theta \in \Theta \text{ and for all } j \in \{1, \dots, n\} \right. \\ \left. V_\theta^{(j)}(\mathbf{h}_{t+1}) = f_\theta([V_\theta^{(1)}(\mathbf{h}_t), \dots, V_\theta^{(n)}(\mathbf{h}_t)], \mathbf{o}_{t+1}) \text{ when } P(\mathbf{h}_t, \mathbf{h}_{t+1} = \mathbf{h}_t a_t \mathbf{o}_t) > 0 \right\} \quad (13)$$

with \mathcal{F}_j the space for $\mathbf{V}_\theta^{(1)}$. Define the projection operator

$$\Pi_{\mathcal{F}_j}(\mathbf{V}) \stackrel{\text{def}}{=} \min_{\hat{\mathbf{V}} \in \mathcal{F}_j} \|\mathbf{V} - \hat{\mathbf{V}}\|_{\mathbf{d}}^2 \quad \text{where } \|\mathbf{V} - \hat{\mathbf{V}}\|_{\mathbf{d}}^2 \stackrel{\text{def}}{=} \sum_{\mathbf{h} \in \mathcal{H}} \mathbf{d}(\mathbf{h})(V(\mathbf{h}) - \hat{V}(\mathbf{h}))^2 \quad (14)$$

where $\mathbf{d} : \mathcal{H} \rightarrow [0, 1]$ is the sampling distribution over histories. Typically, we assume data is generated by following a behavior policy $\mu : \mathcal{H} \rightarrow [0, 1]$, and that \mathbf{d} is the stationary distribution for this policy.

To obtain the projected fixed point solution, a natural goal is to minimize the following projected objective,

$$\min_{\theta \in \Theta} \sum_{j=1}^n \|\Pi_{\mathcal{F}_j}(\mathbf{C}_{\mathbf{V}_\theta}^{(j)} + \mathbf{P}^{(j)}\mathbf{V}_\theta^{(j)}) - \mathbf{V}_\theta^{(j)}\|_{\mathbf{d}}^2 \quad (15)$$

Unfortunately, this objective can be hard to compute, because the projection operator $\Pi_{\mathcal{F}_j}$ onto the nonlinear manifold can be intractable. Instead, we take the same approach as Maei et al. [2010], when defining the nonlinear MSPBE for learning value functions with neural networks and other nonlinear function approximators. The idea is to approximate the projection onto the nonlinear manifold by assuming it is locally linear. Then, we can use a linear projection operator, defined locally at the current set of parameters $\theta \in \Theta$, spanned by the basis $\phi_j(\mathbf{h}) \stackrel{\text{def}}{=} \nabla_\theta \mathbf{V}_\theta^{(j)}(\mathbf{h})$ for all $\mathbf{h} \in \mathcal{H}$. For $\Phi_{\theta,j} = [\phi_j(\mathbf{h}_1), \phi_j(\mathbf{h}_2), \dots, \phi_j(\mathbf{h}_{|\mathcal{H}|})]$ and $\mathbf{D} \stackrel{\text{def}}{=} \text{diag}(\mathbf{d})$

$$\Pi_{\theta,j} = \Phi_{\theta,j}(\Phi_{\theta,j}^\top \mathbf{D} \Phi_{\theta,j})^{-1} \Phi_{\theta,j}^\top \mathbf{D}.$$

As shown in [Maei et al., 2010], even though this uses a locally linear approximation to the objective, fixed points under the original projection are fixed points under this locally linear approximation. It is nonetheless an approximation, as the set of possible fixed points is likely to be larger under this modified projection.

We call the final objective using this projection the MSPBNE², and show in the following lemma, with proof in the appendix, that it can be rewritten in a way that makes it more amenable to compute and sample gradients. We will use this reformulation to develop algorithms to minimize this objective in the next section.

Lemma 1. *The MSPBNE can be written as Equation (16)*

$$\text{MSPBNE}(\theta) \stackrel{\text{def}}{=} \sum_{j=1}^n \|\Pi_{\theta,j}(\mathbf{C}_{\mathbf{V}_\theta}^{(j)} + \mathbf{P}^{(j)}\mathbf{V}_\theta^{(j)}) - \mathbf{V}_\theta^{(j)}\|_{\mathbf{d}}^2 \\ = \mathbb{E} \left[\sum_{j=1}^n \delta_j(H') \phi_{j,\theta}(H) \right]^\top W(\theta)^{-1} \mathbb{E} \left[\sum_{j=1}^n \delta_j(H') \phi_{j,\theta}(H) \right] \quad (16)$$

2. A variant of the MSPBNE has been introduced for TD networks [Silver, 2012]; the above generalizes that MSPBNE to GVF Networks. Because it is a strict generalization, we use the same name.

where

$$W(\boldsymbol{\theta}) \stackrel{\text{def}}{=} \mathbb{E} \left[\sum_{j=1}^n \boldsymbol{\phi}_{j,\boldsymbol{\theta}}(H) \boldsymbol{\phi}_{j,\boldsymbol{\theta}}(H)^\top \right]$$

$$\delta_j(H') \stackrel{\text{def}}{=} \mathbf{C}_{\mathbf{V}_\theta}^{(j)}(H') + \mathbf{P}^{(j)} \mathbf{V}_\theta^{(j)}(H') - \mathbf{V}_\theta^{(j)}(H).$$

From this reformulation, one can see that the MSPBNE objective is a weighted quadratic objective, with weighting matrix $W(\boldsymbol{\theta})$ on vector $\mathbb{E}[\sum_{j=1}^n \delta_j(H') \boldsymbol{\phi}_{j,\boldsymbol{\theta}}(H)]$. The objective is zero—and so minimal—when $\mathbb{E}[\sum_{j=1}^n \delta_j(H') \boldsymbol{\phi}_{j,\boldsymbol{\theta}}(H)] = \mathbf{0}$, which corresponds to the temporal difference (TD) learning fixed point criteria. In fact, TD implicitly optimizes the MSPBE, which corresponds to the above objective with $n = 1$ and fixed features that do not depend on the parameters. Once we have a Projected Bellman Error objective, we can take advantage of the many advances in formulating TD algorithms to optimized MSPBE objectives (see [Ghiassian et al., 2018] for an overview). Therefore, though this objective looks quite complex, there is substantial literature to facilitate minimizing the MSPBNE.

7. Algorithms for the MSPBNE

The algorithms to optimize the MSPBNE are a relatively straightforward combination of standard algorithms for RNNs and the TD algorithms designed to optimize the MSPBE. To provide some intuition on these algorithms, and how to obtain this combination of TD and RNN algorithms, we begin with a simpler setting: extending TD to a recurrent setting, with one GVF. From there, we will introduce a complete algorithm for the MSPBNE, which we call recurrent GTD, and a simpler approximation that we nonetheless find effective in practice.

Consider first the TD update, without recurrence, assuming the true state \mathbf{s}_t at time t is given:

$$\boldsymbol{\theta}_{t+1} \leftarrow \boldsymbol{\theta}_t + \alpha_t \delta_t \nabla_{\boldsymbol{\theta}} V_{\boldsymbol{\theta}}(\mathbf{s}_t) \quad \text{where } \delta_t \stackrel{\text{def}}{=} C_{t+1} + \gamma_{t+1} V_{\boldsymbol{\theta}}(\mathbf{s}_{t+1}) - V_{\boldsymbol{\theta}}(\mathbf{s}_t).$$

For now, we also assume an on-policy setting, and so do not include importance sampling ratios. With recurrence, where the state is estimated and so is a function of $\boldsymbol{\theta}$, the only difference to this update is in the computation of $\nabla_{\boldsymbol{\theta}} V_{\boldsymbol{\theta}}(\mathbf{s}_t)$ where \mathbf{s}_t should instead be thought of $\mathbf{s}_t(\boldsymbol{\theta})$. This gradient now requires the chain rule, to account for the impact of $\boldsymbol{\theta}$ on the last state, and the state before then, and so on:

$$\frac{\partial V_{\boldsymbol{\theta}}(\mathbf{s}_t)}{\partial \boldsymbol{\theta}_i} = \frac{\partial V_{\boldsymbol{\theta}}(\mathbf{s}_t)}{\partial \mathbf{s}_t}^\top \frac{\partial \mathbf{s}_t}{\partial \boldsymbol{\theta}_i}$$

where $\mathbf{s}_t = f_{\boldsymbol{\theta}}(\mathbf{s}_{t-1}, \mathbf{x}_t)$. Computing this gradient back-in-time, $\nabla_{\boldsymbol{\theta}} \mathbf{s}_t$, sometimes called the *sensitivities*, is precisely the aim of most RNN algorithms, including truncated BPTT and RTRL. Any algorithm to compute sensitivities can be used here.

For GVFNs, a recurrent TD update is simpler still, because the value function itself is the state. For the j -th value function—which is the j -th state variable—we get that $\nabla_{\boldsymbol{\theta}} V_{\boldsymbol{\theta}}^{(j)}$ at time t is $\nabla_{\boldsymbol{\theta}} \mathbf{s}_{t,j}$. Notice that this gradient actually corresponds to using the above chain

rule update, by using $V^{(j)}(\mathbf{s}_t) = \mathbf{s}_{t,j}$ as a selector function into the state variable. The **Recurrent TD** update is

$$\begin{aligned}
 \mathbf{s}_t &\leftarrow f_{\boldsymbol{\theta}_t}(\mathbf{s}_{t-1}, \mathbf{x}_t) \\
 \mathbf{s}_{t+1} &\leftarrow f_{\boldsymbol{\theta}_t}(\mathbf{s}_t, \mathbf{x}_{t+1}) \\
 \boldsymbol{\phi}_{t,j} &\leftarrow \nabla_{\boldsymbol{\theta}} \mathbf{s}_{t,j} &> \text{Compute sensitivity using truncated BPTT} \\
 \delta_{t,j} &\leftarrow C_{t+1}^{(j)} + \gamma_{t+1,j} \mathbf{s}_{t+1,j} - \mathbf{s}_{t,j} \\
 \boldsymbol{\theta}_{t+1} &\leftarrow \boldsymbol{\theta}_t + \alpha_t \left[\sum_{j=1}^n \delta_{t,j} \boldsymbol{\phi}_{t,j} \right]
 \end{aligned} \tag{17}$$

The TD update, however, is only an approximate semi-gradient update, even in the fully observable setting. To obtain exact gradient formulas, we turn to Gradient TD (GTD) algorithms. In particular we extend the nonlinear GTD strategy developed by Maei et al. [2010], to the MSPBNE. As above, we will immediately be able to use any algorithm to compute the sensitivities in the Recurrent GTD algorithm. But, the algorithm becomes more complex, simply because nonlinear GTD is more complex than TD even without recurrence.

We can use the following theorem to facilitate estimating the gradient. The main idea is to introduce an auxiliary weight vector, \mathbf{w} , to provide a quasi-stationary estimate of part of the objective. This proof and explicit derivation for the resulting Recurrent TD algorithm is given in the appendix.

Theorem 2. *Assume that $V_{\boldsymbol{\theta}}(\mathbf{h})$ is twice continuously differentiable as a function of $\boldsymbol{\theta}$ for all histories $\mathbf{h} \in \mathcal{H}$ where $\mathbf{d}_{\mu}(\mathbf{h}) > 0$ and that $W(\cdot)$, defined in Equation (25), is non-singular in a small neighbourhood of $\boldsymbol{\theta}$. Then for*

$$\mathbf{w}(\boldsymbol{\theta}) = W(\boldsymbol{\theta})^{-1} \mathbb{E}_{\mu} \left[\sum_{j=1}^n \rho_j(H) \delta_j(H') \boldsymbol{\phi}_{j,\boldsymbol{\theta}}(H) \right] \tag{18}$$

$$\boldsymbol{\psi}(\boldsymbol{\theta}) = \mathbb{E}_{\mu} \left[\sum_{j=1}^n \left(\rho_j(H) \delta_j(H') - \boldsymbol{\phi}_{j,\boldsymbol{\theta}}(H)^{\top} \mathbf{w}(\boldsymbol{\theta}) \right) \nabla^2 V_{j,\boldsymbol{\theta}}(H) \mathbf{w}(\boldsymbol{\theta}) \right] \tag{19}$$

we get the gradient

$$-\frac{1}{2} \nabla \text{MSPBNE}(\boldsymbol{\theta}) = -\mathbb{E}_{\mu} \left[\sum_{j=1}^n \rho_j(H) \nabla_{\boldsymbol{\theta}} \delta_j(H') \boldsymbol{\phi}_{j,\boldsymbol{\theta}}(H)^{\top} \right] \mathbf{w}(\boldsymbol{\theta}) + \boldsymbol{\psi}(\boldsymbol{\theta}) \tag{20}$$

$$= \mathbb{E}_{\mu} \left[\sum_{j=1}^n \rho_j(H) \delta_j(H') \boldsymbol{\phi}_{j,\boldsymbol{\theta}}(H) \right] - \boldsymbol{\psi}(\boldsymbol{\theta}) \tag{21}$$

$$-\mathbb{E}_{\mu} \left[\sum_{j+1}^n \rho_j(H) \left[\sum_{i=1}^n c(j,i) \boldsymbol{\phi}_{i,\boldsymbol{\theta}}(H) + \gamma_j(H') \boldsymbol{\phi}_{j,\boldsymbol{\theta}}(H') \right] \boldsymbol{\phi}_{j,\boldsymbol{\theta}}(H)^{\top} \mathbf{w}(\boldsymbol{\theta}) \right]$$

We now have two additional terms to estimate beyond the standard sensitivities in a typical RNN gradient. First, we need to estimate this additional weight vector \mathbf{w} , given in Equation (18). This can be done using standard techniques in reinforcement learning. Second,

we also need to estimate a Hessian-vector product, given in Equation (19). Fortunately, this can be computed using R-operators, without explicitly computing the Hessian-vector product, using only computation linear in the length of the vector.

The **Recurrent GTD** update is

$$\begin{aligned}
 \mathbf{s}_t &\leftarrow f_{\boldsymbol{\theta}_t}(\mathbf{s}_{t-1}, \mathbf{x}_t) \\
 \mathbf{s}_{t+1} &\leftarrow f_{\boldsymbol{\theta}_t}(\mathbf{s}_t, \mathbf{x}_{t+1}) \\
 \boldsymbol{\phi}_{t,j} &\leftarrow \nabla_{\boldsymbol{\theta}} \mathbf{s}_{t,j} \\
 \boldsymbol{\phi}'_{t,j} &\leftarrow \nabla_{\boldsymbol{\theta}} \mathbf{s}_{t+1,j} \\
 \mathbf{v}_t &= \nabla^2 \mathbf{s}_t(\mathbf{h}_t) \mathbf{w}_t \quad \triangleright \text{Computed using R-operators, see Appendix A.2} \\
 \boldsymbol{\psi}_t &= \sum_{j=1}^n (\rho_j(\mathbf{h}_t) \delta_j(\mathbf{h}_t) - \boldsymbol{\phi}_{j,t}^\top \mathbf{w}_t) \mathbf{v}_t \tag{22} \\
 \boldsymbol{\theta}_{t+1} &= \boldsymbol{\theta}_t + \alpha_t \left[\sum_{j=1}^n \rho_{j,t} \delta_{j,t} \boldsymbol{\phi}_{j,t} - \rho_{j,t} \left[\sum_{i=1}^n c(j,i) \boldsymbol{\phi}'_{i,t} + \gamma_{j,t+1} \boldsymbol{\phi}'_{j,t} \right] \boldsymbol{\phi}_{j,t}^\top \mathbf{w}_t - \boldsymbol{\psi}_t \right] \\
 \mathbf{w}_{t+1} &= \mathbf{w}_t + \beta_t \left[\sum_{j=1}^n \rho_{j,t} \delta_{j,t} \boldsymbol{\phi}_{j,t} - \left(\boldsymbol{\phi}_{j,t}^\top \mathbf{w}_t \right) \boldsymbol{\phi}_{j,t} \right]
 \end{aligned}$$

The derivation for this algorithm is similar to the derivation for Gradient TD Networks Silver [2012], though for this more general setting with GVF Networks. We include additional algorithm details and derivations in Appendix A.1.

As alluded to, there are a variety of possible strategies to optimize the MSPBNE for GVFNs. This variety arises from different strategies to optimize RNNs, back-in-time, as well as from the variety of strategies to optimize the MSPBE for value estimation. For example, we can compute sensitivities using truncated BPTT or RTRL and its many approximations. Similarly, for the MSPBE, there are a variety of different strategies to approximate gradients, because the gradient is not straightforward to sample. These including a variety of gradient TD methods—such as GTD and GTD2—saddlepoint methods and semi-gradient TD (see [Ghiassian et al., 2018] for a more exhaustive list).

In our experiments below, we will also consider the simplest approximate algorithm: Recurrent TD with no back-propagation through time. This algorithm is not a sound gradient descent strategy on the MSPBNE. Instead, it only adjusts parameters to minimize immediate TD-error. However, by incorporating traces, we can obtain credit assignment back-in-time. The TD-error on this step can be attributed to state values back-in-time, with the **TD(λ) algorithm**

$$\begin{aligned}
 \mathbf{s}_t &\leftarrow f_{\boldsymbol{\theta}_t}(\mathbf{s}_{t-1}, \mathbf{x}_t) \\
 \mathbf{s}_{t+1} &\leftarrow f_{\boldsymbol{\theta}_t}(\mathbf{s}_t, \mathbf{x}_{t+1}) \\
 \mathbf{g}_{t,j} &\leftarrow \nabla_{\boldsymbol{\theta}_j} f_{\boldsymbol{\theta}_t}(\mathbf{s}_{t-1}, \mathbf{x}_t) \quad \triangleright \text{gradient given } \mathbf{s}_{t-1}, \text{ no BPTT} \\
 \mathbf{e}_{t,j} &\leftarrow \mathbf{g}_{t,j} + \gamma_{t,j} \lambda \mathbf{e}_{t-1,j} \quad \triangleright \text{eligibility trace, } 0 \leq \lambda \leq 1 \\
 \delta_{t,j} &\leftarrow C_{t+1}^{(j)} + \gamma_{t+1,j} \mathbf{s}_{t+1,j} - \mathbf{s}_{t,j} \\
 \boldsymbol{\theta}_{t+1,j} &\leftarrow \boldsymbol{\theta}_{t,j} + \alpha_t \delta_{t,j} \mathbf{e}_{t,j} \tag{23}
 \end{aligned}$$

Notice the difference to Recurrent TD and Recurrent GTD, that the weights for each GVF are updated independently. This difference arises because the gradient computations for back-in-time, for the sensitivities, is what couples the updates. Without these sensitivities, the immediate gradient of the value $\mathbf{g}_{t,j}$ is independent for each GVF.

8. Connection to other predictive state approaches

The idea that an agent’s knowledge might be represented as predictions has a long history in machine learning. The first references to such a predictive approach can be found in the work of Cunningham [1972], Becker [1973], and Drescher [1991] who hypothesized that agents would construct their understanding of the world from interaction, rather than human engineering. These ideas inspired work on predictive state representations (PSRs) [Littman et al., 2001], as an approach to modeling dynamical systems. Simply put, a PSR can predict all possible interactions between an agent and its environment by reweighting a minimal collection of core test (sequence of actions and observations) and their predictions without the need for a finite history or dynamics model. Extensions to high-dimensional continuous tasks have demonstrated that the predictive approach to dynamical system modeling is competitive with state-of-the-art system identification methods [Hsu et al., 2012]. PSRs can be combined with options [Wolfe and Singh, 2006], and preliminary work suggests discovery of the core tests is possible [McCracken and Bowling, 2005]. One important limitation of the PSR formalism is that the agent’s internal representation of state must be composed exclusively of probabilities of observation sequences.

A PSR can be represented as a GVF network by using myopic $\gamma = 0$ and compositional predictions. For a test $a_1\mathbf{o}_1$, for example, to compute the probability of seeing \mathbf{o}_1 , the cumulant is 1 if \mathbf{o}_1 is observed and 0 otherwise. To get a longer test, say $a_0\mathbf{o}_0a_1\mathbf{o}_1$, a second GVF can be added which predicts the output of the first GVF (i.e., the probability of seeing \mathbf{o}_1 given a_1 is taken), with fixed action a_0 . This equivalence is only for computing probabilities of sequences of observations, given sequences of actions. GVF Networks specify the question, not the answer, and so GVF Networks do not encompass the discovery methods or other nice mathematical properties of PSRs, such as can be obtained with linear PSRs.

TD networks [Sutton and Tanner, 2004] were introduced after PSRs, and inspired by their approach to state construction grounded in observations. GVFNs build directly on the earlier predictive approach called TD networks, and are a strict generalization of TD networks. A TD network [Sutton and Tanner, 2004] is similarly composed of n predictions, and updates using the current observation and previous step predictions like an RNN. TD networks with options [Rafols et al., 2005] condition the predictions on temporally extended actions similar to GVF Networks, but do not incorporate several of the recent modernization of GVFs, including state-dependent discounting and convergence off-policy training methods. The key differences, then, between GVF Networks and TD networks is in how the question networks are expressed and subsequently how they can be answered. GVF Networks are less cumbersome to specify, because they use the language of GVFs. Further, once in this language, it is more straightforward to apply algorithms designed for learning GVFs.

More recently, there has been an effort to combine the benefits of PSRs and RNNs. This began with work on Predictive State Inference Machines (PSIMs) [Sun et al., 2016], for inference in linear dynamical systems. The state is learned in a supervised way, by

using statistics of the future k observations as targets for the predictive state. This earlier work focused on inference in linear dynamical systems, and did not state a clear connection to RNNs. Later work more explicitly combines PSRs and RNNs [Downey et al., 2017, Choromanski et al., 2018], but restricts the RNN architecture to a bilinear update to encode the PSR update for predictive state. In parallel, Venkatraman et al. [2017] proposed another strategy to incorporate ideas from PSRs into RNNs, without restricting the RNN architecture, called Predictive State Decoders (PSDs) [Venkatraman et al., 2017]. Instead of constraining internal state to be predictions about future observations, statistics about future observations are used as auxiliary tasks in the RNN.

Of all these approaches, the most directly related to GVFNs is PSIMs. This connection is most clear from the PSIM objective [Sun et al., 2016, Equation 8], where the goal is to make predictive state match a vector of statistics about future outcomes. There are some key differences, mainly due to a focus on offline estimation in PSIMs. The predictive questions in PSIMs are typically about observations 1-step, 2-step up to k -steps into the future. To use such targets, batches of data need to be gathered and statistics computed offline to create the targets. Further, the state-update (filtering) function is trained using an alternating minimization strategy, with an algorithm called DAgger, rather than with algorithms for RNNs. Nonetheless, the motivation is similar: using an explicit objective to encourage internal state to be a predictive state. A natural question, then, is whether the types of questions used by GVFNs provides advantages over PSIMs. Unlike k -step predictions in the future, GVFs allow questions about outcomes infinitely far into the far, through the use of cumulative discounted sums. Such predictions do not provide high precision about such future events, but nonetheless enable different outcomes to be modelled.

9. Experiments in Forecasting

In this section, we investigate the performance of GVFNs and RNNs on three difficult time series prediction datasets. Time series prediction involves predicting future values of a time-dependent signal, where at each time-step t the agent receives a scalar $y(t)$ and must predict $y(t+h)$ with $h \geq 1 \in \mathbb{N}$. Because only a scalar value is provided, the model is required to represent temporal dependencies starved of other signals. This requires state construction. We show a GVFN optimized *without* BPTT can achieve comparable performance to a GRU network optimized with BPTT.

As we are concerned with online prediction, we asses both approaches with a single pass through the training data. All parameters are tuned using a validation set separate from a testing set with data split with 60% of the data going to training, 20% to validation, and 20% to testing. Parameters are tuned using the average NRMSE on the validation set, and final performance is reported on the testing set.

The architecture we use consists of a GVFN with linear activations followed by another fully-connected linear layer. The GVFs in the GVFN all consist of a constant continuation function with the signal used for prediction as the cumulant. We train the GVFN using TD($\lambda = 0$) (equation 23) ³ with a constant learning rate and a batch size of 32 The linear output layer is trained using Adam, minimizing the mean squared error between

3. It is implied by using TD(0) we are setting the truncation parameter in p-BPTT to $p = 1$. This means we are not using any gradient flow through time to train the GVFN.

the prediction $\hat{y}(t)$ and target $y(t+h)$. We used a grid search tuning strategy with the following hyperparameters: number of GVFS $n \in [32, 64, 128]$, the learning rate for the GVFN $\alpha_{GVFN} = 10^{-k}$ with $k \in [1, \dots, 5]$, and the learning rate for the prediction layer $\alpha_{pred} = 10^{-k}$ with $k \in [1, \dots, 5]$.

The RNN architecture used is comprised of a GRU ⁴ cell followed by a linear prediction layer. We trained the RNN using p-BPTT to minimize the mean squared error. We train the network using the Adam optimizer with a batch size of 32. We follow the same strategy as above to tune the hyperparameters: number of hidden units $n \in [32, 64, 128]$, learning rate $\alpha = 10^{-k}$ with $k \in [2, 3, 4]$, and truncation length $p = 2^k$ with $k \in [0, \dots, 6]$.

9.1 Datasets

We consider three time series previously studied in a comparative analysis of RNN architectures by Bianchi et al. [2017]: the Mackey-Glass time series (previously introduced), the Multiple Superimposed Oscillator, and a real-world electrical load time series.

Multiple Superimposed Oscillator (MSO) the MSO synthetic time series [Jaeger and Haas, 2004] is defined by the sum of four sinusoids with unique frequencies

$$y(t) = \sin(0.2t) + \sin(0.311t) + \sin(0.42t) + \sin(0.51t). \quad (24)$$

The resulting oscillator has a long period of $2000\pi \sim 6283.19$. Because we generate data using $t \in \mathbb{N}$, the oscillator effectively never returns to a previously seen state. These two attributes make prediction difficult with the MSO, as the model cannot rely on memory alone to make good predictions. We generate 1,000,000 samples online and make predictions with a forecast horizon of $h = 10$.

ACEA electrical load dataset the ACEA dataset is a single-variable time series of 137376 energy consumption measurements from an energy provider in Rome. This dataset was originally studied and analyzed by Bianchi et al. [2015], who provided us with the dataset. We make predictions with horizon $h = 144$, which is approximately 24-hours into the future. We apply a unity-based normalization for the input to both networks ⁵, estimating the max/min observation values online. However, we do not apply seasonal differencing; in an online learning system it is unlikely the model will have the prior-knowledge needed to apply seasonal differencing.

9.2 Results

The results shown in figure 4 and table 1 provide compelling evidence of the success of GVFNs in an online time-series setting. The learning curves report the online performance of the models, while the table reports generalization error. The GVFN achieves better performance on the MSO and ACEA datasets as compared to the best performing GRUs, even without BPTT. This could be the extended periodicity and the far horizon predictions of the MSO and ACEA datasets respectively. The truncation parameter needs to be longer, resulting in computation unreasonable for an online agent. While the GVFN generally outperformed

4. We use the standard implementation found in Pytorch (CITE Tensorflow).

5. While we use normalization for both networks to ensure validity in our experiments, we found the GVFN architecture to be robust without normalizing the inputs.

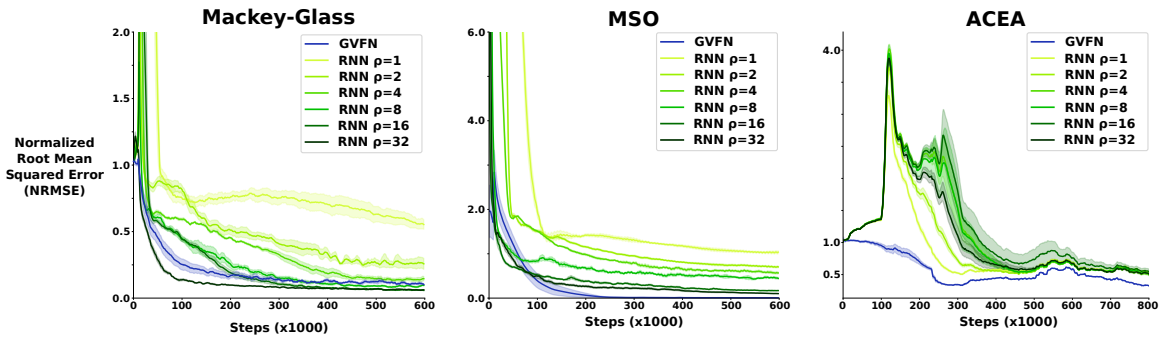


Figure 4: Learning curves for the three time-series datasets. Errors are calculated using the NRMSE averaged over the previous 15000 steps ± 1 standard error over 6 independent runs and sub-sampled every τ_* steps. **(left)** Mackey-Glass ($\tau_{MG} = 100$) (restated from above) **(middle)** Multiple Superimposed Oscillator ($\tau_{MSO} = 100$) **(right)** ACEA electrical load ($\tau_{ACEA} = 10$).

	Mackey-Glass	MSO	ACEA
GVFN	0.1281 ± 0.0182	0.0098 ± 0.0012	0.3797 ± 0.0022
RNN trunc=1	0.5328 ± 0.0270	1.0158 ± 0.0466	0.5512 ± 0.0359
RNN trunc=2	0.3000 ± 0.0536	0.7416 ± 0.0209	0.5354 ± 0.0290
RNN trunc=4	0.1172 ± 0.0128	0.6160 ± 0.0320	0.5491 ± 0.0223
RNN trunc=8	0.0928 ± 0.0142	0.3428 ± 0.0204	0.5267 ± 0.0113
RNN trunc=16	0.0601 ± 0.0087	0.7324 ± 0.1207	0.5518 ± 0.0476
RNN trunc=32	0.0489 ± 0.0054	0.1331 ± 0.0081	0.5517 ± 0.0160

Table 1: Average test NRMSE ± 1 standard error over 6 runs

the GRU on the MSO and ACEA datasets, the GRU was able to better predict on the Mackey-Glass set. The GRU with $p = 8$ performs on par to the GVFN, and out predicts the GVFN with greater truncation.

In addition to good online performance during training, it is also important that the model generalizes well to unseen data. Table 1 shows the average NRMSE over the test set for each of the learners. The results are consistent with the performance on the training set, showing that the GVFN predictions generalize well to unseen data.

10. Investigating Long Temporal Dependencies

In this section, we compare RNNs and GVFNs in a prediction task with long temporal dependencies. We use the Compass World (see Figure 2) to test both approaches. One key feature of this domain is the temporal dependencies can be very long, because the random behavior can stay in the center of the world for many steps, observing only the color white. The observation is encoded with two bits per color: one to indicate the agent observes that color, and the other to indicate another color is observed. The behavior policy chooses randomly between moving one-step forward; turning right/left for one step; moving forward

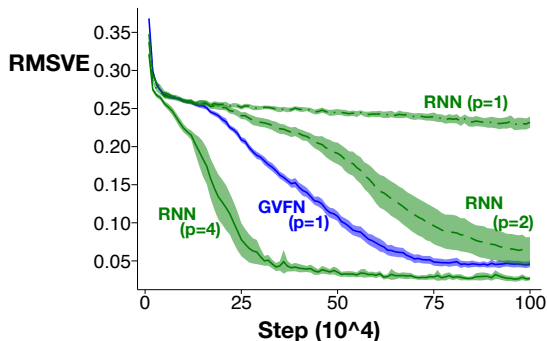


Figure 5: Learning curves in Compass World comparing RNNs and GVFNs. The GVFN was able to learn with one-step update, with $p = 1$, while the RNNs required at least $p = 2$ to learn with much better performance with higher truncation. While not shown here, a GRU requires $p = 8$ to learn. Learning rates were swept over a range of $\{\min(0.1 * 1.5^{-i}, 1.0); i \in -6, 6\}$, with the best over the entire trajectory used in the final plot.

until the wall is reached (*leap*); or randomly selecting actions for k steps (*wander*). The full observation vector is encoded based on which action was taken, and includes a bias unit.

We chose five hard-to-learn GVFNs with predictions corresponding to the wall the agent is facing. These predictions are not learnable without constructing an internal state. These five questions correspond to leap questions. The leap question is defined as having a cumulant of 1 in the event of seeing a specific wall (orange, yellow, red, blue, green), and a termination function defined as $\gamma = 0$ when the wall is seen and $\gamma = 1$ otherwise.

We use the same architecture for both RNNs and GVFNs, where we modify a simple recurrent cell to account directly for the action the agent just performed. This is done by specifying separate weight vectors $w_a \in \mathbb{R}^n, a \in \mathcal{A}$ for each action the agent can take. The hidden state is then calculated as $\mathbf{s}_{t+1} = \sigma(w_{a_t}^\top [\mathbf{x}_{t+1}, \mathbf{s}_t])$, where σ is the activation function. Another option is to simply pass the action to the network. Our architectural choice, having separate components inside the RNN, significantly improved the performance of both the RNN and the GVFN. For the GRUs, we pass the action as a one-hot encoding, because this architectural modification is less straightforward. For RNNs, we use the hyperbolic tangent and the sigmoid function for GVFNs. We used sigmoids instead for GVFNs, because the returns are always nonnegative; otherwise, these two activations represent a similar architectural choice.

We also have to specify the GVFNs for the GVFN. We use a set of GVFNs based on similar questions specified for TD Networks for this problem [Rafols et al., 2005]. The expert network is defined similarly for the 5 colours: 3 GVFNs with a persistent policy (one for each of the 3 available actions), myopic termination, and a cumulant of the colour bit; 1 leap GVFN with cumulant of the colour; 2 GVFNs with a persistent policy (left, right) with myopic termination and a cumulant of the previous leap GVFNs; 2 leap GVFNs with cumulants of the previous myopic GVFNs; 1 GVFN with uniform random policy with $\gamma = 0$ at a wall event and $\gamma = 0.5$ otherwise.

Figure 5 contains the results of the best performing parameters for the GVFN with $p = 1$, and the RNNs for $p \in \{1, 2, 4\}$. The RNN performs quite well, but still requires a small amount of BPTT. While not shown here, GRUs perform well with a truncation parameter $p = 8$. The first surprising result is how effectively all the RNNs learn in this domain, despite the relatively long dependencies back-in-time. Despite the fact that RNNs do not have that much sensitivity to p , it is clear that GVFNs reduce sensitivity to p . This provides some

evidence that GVFNs are robust to truncation length, as well as some evidence for the predictive representation hypothesis.

11. Investigating Poorly Specified GVFNs

In all experiments until now, GVFNs were robust to truncation back-in-time. In fact, computing one-step gradients was sufficient for good performance. A natural question is when we can expect this to fail. We hypothesize that this robustness to truncation relies on appropriately specifying the GVFs in the GVFN. Poorly specified GVFs could both (a) make it so that the GVFN is incapable of constructing a state that can accurately predict the target and (b) make training difficult or unstable.

In this section, we test GVFNs with two sets of poorly specified GVFs, in a simple environment called Ring World. This environment resembles the Cycle World, for which there is some empirical evidence that TD Networks require p-BPTT [Silver, 2012]. Because TD Networks are subsumed by GVFNs—every TD Network can be specified as a GVFN—this implies there are known settings of GVFNs where $p > 1$ is needed in training. We re-examine this result in a slightly more complex domain, to enable a few more natural choices of GVFs in the GVFN.

Ring World is a six-state domain [Tanner and Sutton, 2005] where the agent can move left or right in the ring. All the states are indistinguishable except state six. The observation vector is simply a two bit binary encoding indicating if the agent is state six or not. The agent behaves uniformly randomly. The goal is to predict the observation bit on the next time step.

We define two GVFNs, both with similar attributes but with empirically varying optimization difficulties. The first GVFN (Gamma Chain) arranges 14 GVFs into two mirrored networks for each action. These networks are constructed in a similar manner as the chained TDN architecture in [Silver, 2012] with an added GVF. The first GVF is a myopic prediction of the observed bit. Subsequent GVFs make myopic predictions of the priors prediction (i.e. the cumulant for v_t^i is v_{t+1}^{i-1} where the cumulant for $i = 0$ is the observed bit). A final GVF is added with a cumulant of the observed bit and continuation function of $\gamma = 0$ when the observed bit is active and $\gamma = 0.9$ otherwise. As mentioned, this network is mirrored for the two policies which deterministically select one of the actions. The GVFN is then fed into a linear prediction layer predicting the observed bit on the next step. The second GVFN (Half Chain) only specifies 6 GVFs chained as previously specified for a single action.

We present results for Recurrent TD; the conclusions hold for Recurrent GTD as well. We include an RNN for baseline performance, with the same dimension $n = 14$. The goal here is not to improve on the RNN, but rather to understand GVFNs under poor specification of GVFs. We sweep over learning rates for all methods tested selecting the best parameter setting for overall performance.

Figure 6 shows the results of the Ring World experiments. The main take-away is that for these poorly specified GVFNs, $p > 1$ was necessary to obtain reasonable performance. The Gamma Chain required $p \geq 2$ and the Half Chain, which is an even worse specification than the Gamma Chain, required $p \geq 4$. The RNN, on the other hand, required $p \geq 2$ and learned much more quickly than both GVFNs.

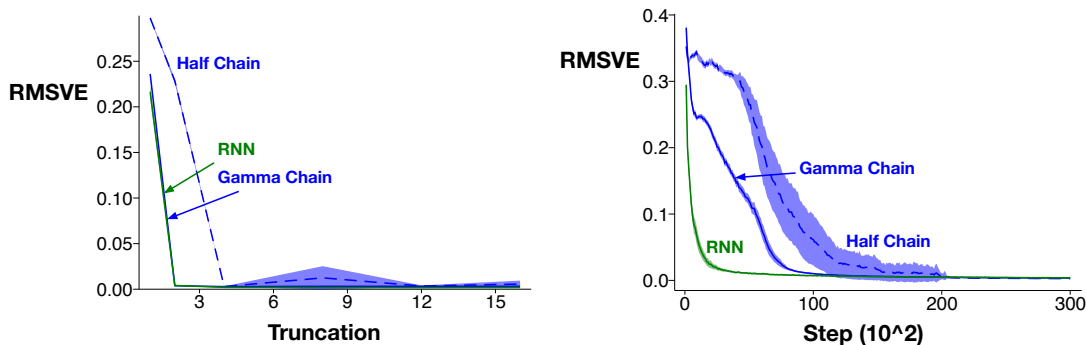


Figure 6: **(left)** Sensitivity to truncation level in Ring World for the RMSVE over the final 50,000 steps. **(right)** Learning curves in Ring World of RNN $p = 2$, GVFN Gamma Chain $p = 2$, GVFN Half Chain $p = 4$. These learning curves are the smallest to make the hard-to-learn questions learnable.

The experiments in these last two sections were designed to carefully highlight properties of GVFNs. The time series experiments showed that GVFs have the potential to be effective, outside of the simple toy domains designed to understand predictive representations. Nonetheless, the results in this work remain limited to relatively simple settings. A clear next step is to verify the properties of GVFNs suggested by our experiments, in a wider variety of settings.

12. Discussion and Conclusions

In this work, we made a case for a new recurrent architecture, called GVF Networks. GVFNs constrain the hidden layer to correspond to predictions about the future, and so can be seen as a regularized or constrained RNN architecture. We first derive a sound fixed-point objective for these networks. We then show in experiments that GVFNs can outperform GRUs, without requiring gradients to be compute (far) back in time. We demonstrated that this is particularly true for GVFNs with an expert set of GVF questions, but that good performance could also be obtained with a naive generation strategy for GVFs—still outperforming the best GRU model.

An important limitation of this work is that we assumed that the GVFs for the GVFN were given. A critical question to make these RNNs easy-to-use is to answer the discovery question: how to autonomously discover these questions. The discovery problem is an important next step, and beyond the scope of this work. We can, however, provide some rules of thumb for choosing GVFs today, without yet having an answer to the discovery question. In our time-series experiments, we found selecting GVFs with constant $\gamma^{(j)} \in [1 - 2^{-j}]$ to be surprisingly effective across the settings with fixed policies—namely the time series datasets. We also see good results with a random generation strategy, generating GVFs from a set of simpler primitives (see Appendix B).

Finally, in this work, we constrained ourselves to GVFNs where all hidden states are predictions. A natural extension is to consider a GVFN that only constrains certain hidden states to be predictions and otherwise allows other states to simply be set to improve prediction accuracy for the targets. This modification could provide the improved stability

of GVFNs, but improve representability. Additionally, GVFNs could even be combined with other RNN types, like LSTMs, by simply concatenating the states learned by the two RNN types. Overall, GVFNs provide a complementary addition to the many other RNN architectures available, particularly for continual learning systems with long temporal dependencies; with this work, we hope to expand interest and investigation further into these promising RNN models.

References

- Leonard E Baum and Ted Petrie. Statistical Inference for Probabilistic Functions of Finite State Markov Chains. *The Annals of Mathematical Statistics*, 1966.
- Joseph D Becker. A model for the encoding of experiential information. *Computer Models of Thought and Language*, 1973.
- Filippo Maria Bianchi, Enrico De Santis, Antonello Rizzi, and Alireza Sadeghian. Short-Term Electric Load Forecasting Using Echo State Networks and PCA Decomposition. *IEEE Access*, 2015.
- Filippo Maria Bianchi, Enrico Maiorino, Michael C Kampffmeyer, Antonello Rizzi, and Robert Jenssen. An overview and comparative analysis of Recurrent Neural Networks for Short Term Load Forecasting. *arXiv:1705.04378*, 2017.
- B Boots, S.M. Siddiqi, and G.J. Gordon. Closing the learning-planning loop with predictive state representations. *The International Journal of Robotics Research*, 2011.
- Kyunghyun Cho, Bart van Merriënboer, Dzmitry Bahdanau, and Yoshua Bengio. On the Properties of Neural Machine Translation: Encoder-Decoder Approaches. In *International Conference on Machine Learning*, 2014.
- Krzysztof Choromanski, Carlton Downey, and Byron Boots. Initialization matters: Orthogonal Predictive State Recurrent Neural Networks. In *International Conference on Learning Representations*, 2018.
- Michael Cunningham. *Intelligence: Its Organization and Development*. Academic Press., 1972.
- Carlton Downey, Ahmed Hefny, Byron Boots, Geoffrey J Gordon, and Boyue Li. Predictive State Recurrent Neural Networks. In *Advances in Neural Information Processing Systems*, 2017.
- Gary L Drescher. *Made-up minds: a constructivist approach to artificial intelligence*. MIT press, 1991.
- H Durrant-Whyte and Tim Bailey. Simultaneous localization and mapping. *IEEE Robotics and Automation Magazine*, 2006.
- Sina Ghiassian, Andrew Patterson, Martha White, Richard S Sutton, and Adam White. Online Off-policy Prediction. *arXiv:1811.02597*, 2018.

- Sepp Hochreiter and Jürgen Schmidhuber. Long Short-Term Memory. *Neural Computation*, 1997.
- J J Hopfield. Neural Network and Physical Systems with Emergent Collective Computational Abilities. *Proceedings of the National Academy of Sciences of the United States of America*, 1982.
- D Hsu, SM Kakade, and Tong Zhang. A spectral algorithm for learning Hidden Markov Models. *Journal of Computer and System Sciences*, 2012.
- Max Jaderberg, Volodymyr Mnih, Wojciech Marian Czarnecki, Tom Schaul, Joel Z Leibo, David Silver, and Koray Kavukcuoglu. Reinforcement learning with unsupervised auxiliary tasks. *arXiv:1611.05397*, 2016.
- Herbert Jaeger and Harald Haas. Harnessing Nonlinearity: Predicting Chaotic Systems and Saving Energy in Wireless Communication. *Science*, 2004.
- Leslie Pack Kaelbling, Michael L Littman, and A R Cassandra. Planning and acting in partially observable stochastic domains. *Artificial intelligence*, 1998.
- Long-Ji Lin and Tom M Mitchell. Reinforcement learning with hidden states. In *International Conference on Simulation of Adaptive Behavior*, 1993.
- Michael L Littman, Richard S Sutton, and S Singh. Predictive representations of state. In *Advances in Neural Information Processing Systems*, 2001.
- L Ljung. Perspectives on system identification. *Annual Reviews in Control*, 2010.
- H Maei. *Gradient Temporal-Difference Learning Algorithms*. PhD thesis, University of Alberta, 2011.
- H Maei, C Szepesvári, S Bhatnagar, and R Sutton. Toward Off-Policy Learning Control with Function Approximation. In *International Conference on Machine Learning*, 2010.
- R A McCallum. Learning to use selective attention and short-term memory in sequential tasks. In *International Conference on Simulation of Adaptive Behavior*, 1996.
- P McCracken and Michael H Bowling. Online discovery and learning of predictive state representations. In *Advances in Neural Information Processing Systems*, 2005.
- Joseph Modayil, Adam White, and Richard S Sutton. Multi-timescale nexting in a reinforcement learning robot. *Adaptive Behavior*, 2014.
- Razvan Pascanu, Tomas Mikolov, and Yoshua Bengio. On the difficulty of training recurrent neural networks. In *International Conference on Machine Learning*, 2013.
- Barak A Pearlmutter. Fast Exact Multiplication by the Hessian. *Neural Computation*, 1994.
- Eddie J Rafols, Mark B Ring, Richard S Sutton, and Brian Tanner. Using predictive representations to improve generalization in reinforcement learning. In *International Joint Conference on Artificial Intelligence*, 2005.

- M Rudary, S Singh, and D Wingate. Predictive linear-Gaussian models of stochastic dynamical systems. In *Conference on Uncertainty in Artificial Intelligence*, 2005.
- Tom Schaul and Mark Ring. Better generalization with forecasts. In *International Joint Conference on Artificial Intelligence*, 2013.
- D Silver. Gradient Temporal Difference Networks. In *European Workshop on Reinforcement Learning*, 2012.
- W Sun, A Venkatraman, B Boots, and J. Andrew Bagnell. Learning to filter with predictive state inference machines. In *International Conference on Machine Learning*, 2016.
- Richard S Sutton and Brian Tanner. Temporal-Difference Networks. In *Advances in Neural Information Processing Systems*, 2004.
- Richard S Sutton, J Modayil, M Delp, T Degris, P.M. Pilarski, A White, and D Precup. Horde: A scalable real-time architecture for learning knowledge from unsupervised sensorimotor interaction. In *International Conference on Autonomous Agents and Multiagent Systems*, 2011.
- B Tanner and Richard S Sutton. Temporal-Difference Networks with History. In *International Joint Conference on Artificial Intelligence*, 2005.
- Hado van Hasselt and Richard S Sutton. Learning to predict independent of span. *arXiv:1508.04582*, 2015.
- Arun Venkatraman, Nicholas Rhinehart, Wen Sun, Lerrel Pinto, Martial Hebert, Byron Boots, Kris Kitani, and J Bagnell. Predictive-State Decoders: Encoding the Future into Recurrent Networks. *Proceedings of the 31st International Conference on Neural Information Processing Systems*, 2017.
- Christopher M Vigorito. Temporal-Difference Networks for Dynamical Systems with Continuous Observations and Actions. In *Conference on Uncertainty in Artificial Intelligence*, 2009.
- Ronald J Williams and David Zipser. A Learning Algorithm for Continually Running Fully Recurrent Neural Networks. *Neural Computation*, 1989.
- D Wingate and S Singh. Mixtures of predictive linear gaussian models for nonlinear, stochastic dynamical systems. In *AAAI Conference on Artificial Intelligence*, 2006.
- Britton Wolfe and Satinder P Singh. Predictive state representations with options. In *International Conference on Machine Learning*, 2006.

Appendix A. Algorithmic Details and Derivations

In this section we provide the derivation of Recurrent-GTD from the MSPBNE, including off-policy corrections, and the details in recursively calculating the gradients of a GVFN back through time using an RTRL derivation, with details easily extended to BPTT.

A.1 Deriving Recurrent-GTD

While the MSPBNE has been derived for on-policy prediction questions, the extension to off-policy prediction is straightforward using the importance ratio.

Lemma 2. *Assume the behaviour policy μ has stationary distribution $\mathbf{d}_\mu(\mathbf{h}) > 0$ for all $\mathbf{h} \in \mathcal{H}$ where $\mathbf{d}_{\pi_j}(\mathbf{h}) > 0$ for any of the policies π_1, \dots, π_n . Assume that for $j \in \{1, \dots, n\}$ that $V_{j,\theta}(\mathbf{h})$ is continuously differentiable as a function of θ for all histories $\mathbf{h} \in \mathcal{H}$ where $\mathbf{d}_\mu(\mathbf{h}) > 0$ and that the matrix*

$$W(\theta) \stackrel{\text{def}}{=} \mathbb{E}_\mu \left[\sum_{j=1}^n \phi_{j,\theta}(H) \phi_{j,\theta}(H)^\top \right] = \sum_{\mathbf{h} \in \mathcal{H}} \mathbf{d}_\mu(\mathbf{h}) \sum_{j=1}^n \phi_{j,\theta}(\mathbf{h}) \phi_{j,\theta}(\mathbf{h})^\top \in \mathbb{R}^{p \times p} \quad (25)$$

is nonsingular, where H represents a random vector for the history in the expectation. Then for importance sampling ratios $\rho_j(\mathbf{h}) = \frac{\pi_j(\mathbf{h})}{\mu(\mathbf{h})}$, and TD-errors $\delta_j(\mathbf{h}')$

$$\begin{aligned} & \text{MSPBNE}(\theta) \\ &= \mathbb{E}_\mu \left[\sum_{j=1}^n \rho_j(H) \phi_{j,\theta}(H) \delta_j(H') \right]^\top W(\theta)^{-1} \mathbb{E}_\mu \left[\sum_{j=1}^n \rho_j(H) \phi_{j,\theta}(H) \delta_j(H') \right] \end{aligned} \quad (26)$$

where H' is a history immediately following history H .

Proof. The extension is a relatively straightforward modification of the nonlinear MSPBE [Maei, 2011] and the TD-network MSPBNE [Silver, 2012]. The main modification is in the extension to off-policy sampling—both allowing different π_j and necessitating the addition of importance sampling ratio—and the extension to transition-based discounting. ■

With lemma 2 we can rewrite the MSPBNE fully into expectation form to more easily take the gradient with respect to θ .

Lemma 3. *We can rewrite the MSPBNE as*

$$\begin{aligned} & \text{MSPBNE}(\theta) \\ &= \mathbb{E}_\mu \left[\sum_{j=1}^n \rho_j(H') \phi_{j,\theta}(H) \delta_j(H') \right]^\top W(\theta)^{-1} \mathbb{E}_\mu \left[\sum_{j=1}^n \rho_j(H') \phi_{j,\theta}(H) \delta_j(H') \right] \end{aligned} \quad (27)$$

where

$$\begin{aligned} W(\theta) &\stackrel{\text{def}}{=} \mathbb{E}_\mu \left[\sum_{j=1}^n \phi_{j,\theta}(H) \phi_{j,\theta}(H)^\top \right] \\ \delta_j(H') &= \delta_{j,\theta}(H') = \mathbf{C}_{\mathbf{V}_\theta}^{(j)}(H') + \mathbf{P}^{(j)} \mathbf{V}_\theta^{(j)}(H') - \mathbf{V}_\theta^{(j)}(H) \end{aligned}$$

Proof.

$$\begin{aligned}
 \text{MSPBNE}(\boldsymbol{\theta}) &= \sum_{j=1}^n \|\Pi_{\mathcal{F}}(\mathbf{C}_{\mathbf{V}_{\boldsymbol{\theta}}}^{(j)} + \mathbf{P}^{(j)}\mathbf{V}_{\boldsymbol{\theta}}^{(j)}) - \mathbf{V}_{\boldsymbol{\theta}}^{(j)}\|_{\mathbf{d}}^2 \\
 &= \sum_{j=1}^n \|\Pi_{\mathcal{F}}(\mathbf{C}_{\mathbf{V}_{\boldsymbol{\theta}}}^{(j)} + \mathbf{P}^{(j)}\mathbf{V}_{\boldsymbol{\theta}}^{(j)} - \mathbf{V}_{\boldsymbol{\theta}}^{(j)})\|_{\mathbf{d}}^2 \\
 &= \sum_{j=1}^n \|\Pi_{\mathcal{F}}(\delta_j(H'))\|_{\mathbf{d}}^2
 \end{aligned}$$

We can wrap the projection operator around the full TD error for similar reasons as the non-linear TDC algorithms—the values of the prior step should already be on the manifold and the projection does nothing.

We can then decompose this as:

$$\text{MSPBNE}(\boldsymbol{\theta}) = \sum_{j=1}^n (\Pi_{\mathcal{F}}(\delta_j(H')))^\top \mathbf{D} (\Pi_{\mathcal{F}}(\delta_j(H')))^\top$$

The rest of the proof follows similar algebraic operations as prior use of the MSPBNE [Silver, 2012]. ■

Now that the objective is written in its expectation form, the gradients can be take with respect to the weight parameter as shown in 2.

Theorem 2. *Assume that $V_{\boldsymbol{\theta}}(\mathbf{h})$ is twice continuously differentiable as a function of $\boldsymbol{\theta}$ for all histories $\mathbf{h} \in \mathcal{H}$ where $\mathbf{d}_{\mu}(\mathbf{h}) > 0$ and that $W(\cdot)$, defined in Equation (25), is non-singular in a small neighbourhood of $\boldsymbol{\theta}$. Then for*

$$\mathbf{w}(\boldsymbol{\theta}) = W(\boldsymbol{\theta})^{-1} \mathbb{E}_{\mu} \left[\sum_{j=1}^n \rho_j(H) \delta_j(H') \phi_{j,\boldsymbol{\theta}}(H) \right] \quad (18)$$

$$\boldsymbol{\psi}(\boldsymbol{\theta}) = \mathbb{E}_{\mu} \left[\sum_{j=1}^n \left(\rho_j(H) \delta_j(H') - \phi_{j,\boldsymbol{\theta}}(H)^\top \mathbf{w}(\boldsymbol{\theta}) \right) \nabla^2 V_{j,\boldsymbol{\theta}}(H) \mathbf{w}(\boldsymbol{\theta}) \right] \quad (19)$$

we get the gradient

$$-\frac{1}{2} \nabla \text{MSPBNE}(\boldsymbol{\theta}) = -\mathbb{E}_{\mu} \left[\sum_{j=1}^n \rho_j(H) \nabla_{\boldsymbol{\theta}} \delta_j(H') \phi_j(H)^\top \right] \mathbf{w}(\boldsymbol{\theta}) + \boldsymbol{\psi}(\boldsymbol{\theta}) \quad (20)$$

$$= \mathbb{E}_{\mu} \left[\sum_{j=1}^n \rho_j(H) \delta_j(H') \phi_{j,\boldsymbol{\theta}}(H) \right] - \boldsymbol{\psi}(\boldsymbol{\theta}) \quad (21)$$

$$- \mathbb{E}_{\mu} \left[\sum_{j+1}^n \rho_j(H) \left[\sum_{i=1}^n c(j, i) \phi_{i,\boldsymbol{\theta}}(H) + \gamma_j(H') \phi_{j,\boldsymbol{\theta}}(H') \right] \phi_{j,\boldsymbol{\theta}}(H)^\top \mathbf{w}(\boldsymbol{\theta}) \right]$$

Proof. For simplicity in notation below, we drop the explicit dependence on the random variable H in the expectations.

$$\begin{aligned}\phi_{j,\theta}(H) &\rightarrow \phi_{j,\theta}, & \phi_{j,\theta}(H') &\rightarrow \phi'_{j,\theta} \\ \delta_j(H') &\rightarrow \delta'_j, & \rho_j(H) &\rightarrow \rho_j\end{aligned}$$

$$J(\boldsymbol{\theta}) = \mathbb{E}_\mu \left[\sum_{j=1}^n \rho_j \phi_{j,\theta} \delta'_j \right]^\top W(\boldsymbol{\theta})^{-1} \mathbb{E}_\mu \left[\sum_{j=1}^n \rho_j \phi_{j,\theta} \delta'_j \right] \triangleright \text{By Lemma 3}$$

$$\mathbf{w}(\boldsymbol{\theta}) = W(\boldsymbol{\theta})^{-1} \mathbb{E}_\mu \left[\sum_{j=1}^n \rho_j \phi_{j,\theta} \delta'_j \right]$$

$$\nabla_{\boldsymbol{\theta}} \mathbb{E}_\mu \left[\sum_{j=1}^n \rho_j \phi_{j,\theta} \delta'_j \right] = \mathbb{E}_\mu \left[\sum_{j=1}^n \rho_j \nabla_{\boldsymbol{\theta}} \phi_{j,\theta} \delta'_j + \phi_{j,\theta} \nabla_{\boldsymbol{\theta}} \delta'_j \right]$$

$$\nabla_{\boldsymbol{\theta}} W(\boldsymbol{\theta})^{-1} = -W(\boldsymbol{\theta})^{-1} \nabla_{\boldsymbol{\theta}} W(\boldsymbol{\theta}) W(\boldsymbol{\theta})^{-1}$$

$$= -2W(\boldsymbol{\theta})^{-1} \mathbb{E}_\mu \left[\sum_{j=1}^n \nabla_{\boldsymbol{\theta}} \phi_{j,\theta} \phi_{j,\theta}^\top \right] W(\boldsymbol{\theta})^{-1}$$

$$\nabla_{\boldsymbol{\theta}} J(\boldsymbol{\theta}) = 2\mathbb{E}_\mu \left[\sum_{j=1}^n \rho_j \nabla_{\boldsymbol{\theta}} \phi_{j,\theta} \delta'_j + \phi_{j,\theta} \nabla_{\boldsymbol{\theta}} \delta'_j \right]^\top \mathbf{w}(\boldsymbol{\theta})$$

$$- 2\mathbf{w}(\boldsymbol{\theta})^\top \mathbb{E}_\mu \left[\sum_{j=1}^n \nabla_{\boldsymbol{\theta}} \phi_{j,\theta} \phi_{j,\theta}^\top \right] \mathbf{w}(\boldsymbol{\theta})$$

$$-\frac{1}{2}J(\boldsymbol{\theta}) = \mathbf{w}(\boldsymbol{\theta})^\top \mathbb{E}_\mu \left[\sum_{j=1}^n \nabla_{\boldsymbol{\theta}}^2 V_{j,\theta} \phi_{j,\theta}^\top \right] \mathbf{w}(\boldsymbol{\theta})$$

$$- \mathbb{E}_\mu \left[\sum_{j=1}^n \rho_j \nabla_{\boldsymbol{\theta}}^2 V_{j,\theta} \delta'_j \right]^\top \mathbf{w}(\boldsymbol{\theta}) - \mathbb{E} \left[\sum_{j=1}^n \rho_j \phi_{j,\theta} \nabla_{\boldsymbol{\theta}} \delta'_j \right]^\top \mathbf{w}(\boldsymbol{\theta})$$

$$= -\mathbb{E} \left[\sum_{j=1}^n \rho_j \left(\left[\sum_{i=1}^n c(j,i) \phi_{i,\theta} \right] + \gamma'_j \phi_{j,\theta} - \phi_{j,\theta} \right) \phi_{j,\theta}^\top \right] \mathbf{w}(\boldsymbol{\theta})$$

$$- \mathbb{E}_\mu \left[\sum_{j=1}^n \rho_j \nabla_{\boldsymbol{\theta}}^2 V_{j,\theta} \delta'_j \right]^\top \mathbf{w}(\boldsymbol{\theta}) + \mathbf{w}(\boldsymbol{\theta})^\top \mathbb{E}_\mu \left[\sum_{j=1}^n \nabla_{\boldsymbol{\theta}}^2 V_{j,\theta} \phi_{j,\theta}^\top \right] \mathbf{w}(\boldsymbol{\theta})$$

$$= \mathbb{E} \left[\sum_{j=1}^n \rho_j \left(\phi_{j,\theta} - \left(\left[\sum_{i=1}^n c(j,i) \phi_{i,\theta} \right] + \gamma'_j \phi_{j,\theta} \right) \right) \phi_{j,\theta}^\top \right] \mathbf{w}(\boldsymbol{\theta}) - \Psi(\boldsymbol{\theta})$$

$$= \mathbb{E} \left[\sum_{j=1}^n \rho_j \phi_{j,\theta} \delta_j - \rho_j \left(\left[\sum_{i=1}^n c(j,i) \phi_{i,\theta} \right] + \gamma'_j \phi_{j,\theta} \right) \phi_{j,\theta}^\top \right] \mathbf{w}(\boldsymbol{\theta}) - \Psi(\boldsymbol{\theta})$$

■

A.2 Computing gradients of the value function back through time

In this section, we show how to compute ϕ_t , which was needed in the algorithms. For both Backpropagation Through Time or Real Time Recurrent Learning, it is useful to take advantage of the following formula for *recurrent sensitivities*

$$\begin{aligned} \frac{\partial V_i(S_{t+1})}{\partial \theta_{(k,j)}} &= \dot{\sigma}(x_{t+1}^\top \theta_i) \left(\left(\frac{\partial x_{t+1}}{\partial \theta_{(k,j)}} \right)^\top \theta_i + (x_{t+1})_j \delta_{i,k}^\kappa \right) \\ &= \dot{\sigma}(x_{t+1}^\top \theta_i) \left(\left[\mathbf{0}, \frac{\partial V_1(S_t)}{\partial \theta_{(k,j)}}, \dots, \frac{\partial V_n(S_t)}{\partial \theta_{(k,j)}} \right]^\top \theta_i + (x_{t+1})_j \delta_{i,k}^\kappa \right) \end{aligned}$$

where δ^κ is the Kronecker delta function. Given this formula, BPTT or RTRL can simply be applied.

For Recurrent GTD—though not for Recurrent TD—we additionally need to compute the Hessian back in time, for the Hessian-vector product. The Hessian for each value function is a $n((d+n)) \times n((d+n))$ matrix; computing the Hessian-vector product naively would cost at least $O(((d+n)+n)^2 n^2)$ for each GVF, which is prohibitively expensive. We can avoid this using R-operators also known as Pearlmutter’s method [Pearlmutter, 1994]. The R-operator $\mathcal{R}\{\cdot\}$ is defined as

$$\mathcal{R}_{\mathbf{w}} \left\{ \mathbf{g}(\boldsymbol{\theta}) \right\} \stackrel{\text{def}}{=} \left. \frac{\partial \mathbf{g}(\boldsymbol{\theta} + r\mathbf{w})}{\partial r} \right|_{r=0}$$

for a (vector-valued) function \mathbf{g} and satisfies

$$\mathcal{R}_{\mathbf{w}} \left\{ \nabla_{\boldsymbol{\theta}} f(\boldsymbol{\theta}) \right\} = \nabla_{\boldsymbol{\theta}}^2 f(\boldsymbol{\theta}) \mathbf{w}.$$

Therefore, instead of computing the Hessian and then producting with \mathbf{w}_t , this operation can be completed in linear time, in the length of \mathbf{w}_t .

Specifically, for our setting, we have

$$\mathcal{R}_{\mathbf{w}} \left\{ \dot{\sigma}(x_t^\theta) [\nabla x_t^\top \boldsymbol{\theta} + x_t^\top \nabla \boldsymbol{\theta}] \right\} = \left. \frac{\partial}{\partial r} \left(\dot{\sigma}(x_t^\theta) [\nabla x_t^\top \boldsymbol{\theta} + x_t^\top \nabla \boldsymbol{\theta}] \right) \right|_{r=0}$$

To make the calculation more manageable we separate into each partial for every node k and associated weight j .

$$\begin{aligned}
 \frac{\partial V_i(S_{t+1}, \boldsymbol{\theta})}{\partial \boldsymbol{\theta}_{(k,j)}} &= \dot{\sigma}(x_{t+1}^\top \boldsymbol{\theta}_i) (\eta_{t+1})_{j,k} \\
 (\eta_{t+1})_{k,j} &= ((\mathbf{u}_t)_{k,j}^\top \boldsymbol{\theta}_i + (x_{t+1})_j \delta_{i,k}) \\
 (\mathbf{u}_t)_{k,j} &= \left[\mathbf{0}, \frac{\partial V_1(S_t)}{\partial \boldsymbol{\theta}_{(k,j)}}, \dots, \frac{\partial V_n(S_t)}{\partial \boldsymbol{\theta}_{(k,j)}} \right] \\
 \boldsymbol{\xi}_t &= \left[\mathbf{0}, \frac{\partial V_1(S_t)}{\partial r}, \dots, \frac{\partial V_n(S_t)}{\partial r} \right] \\
 (\mathcal{R}_t)_{w,V} &= \left[\mathbf{0}, \mathcal{R}_w \left\{ \frac{\partial V_1(S_{t-1})}{\partial \boldsymbol{\theta}_{(k,j)}} \right\}, \dots, \mathcal{R}_w \left\{ \frac{\partial V_n(S_{t-1})}{\partial \boldsymbol{\theta}_{(k,j)}} \right\} \right] \\
 \mathcal{R}_w \left\{ \frac{\partial V_i(S_{t+1}, \boldsymbol{\theta})}{\partial \boldsymbol{\theta}_{(k,j)}} \right\} &= \frac{\partial^2 V_i(S_{t+1}, \boldsymbol{\theta} + r\mathbf{w})}{\partial r \partial \boldsymbol{\theta}_{(k,j)}} \Big|_{r=0} \\
 &= \ddot{\sigma} \left(x_{t+1}^\top (\boldsymbol{\theta}_i + r\mathbf{w}_i) \right) \left(\boldsymbol{\xi}_t^\top (\boldsymbol{\theta}_i + r\mathbf{w}_i) + x_{t+1}^\top \mathbf{w}_i \right) (\eta_{t+1})_{j,k} \\
 &\quad + \dot{\sigma} \left(x_{t+1}^\top (\boldsymbol{\theta}_i + r\mathbf{w}_i) \right) \left((\mathcal{R}_t)_{w,V}^\top (\boldsymbol{\theta} + r\mathbf{w}) + (\mathbf{u}_t)_{k,j}^\top \mathbf{w}_i + (\boldsymbol{\xi}_t)_j \delta_{k,i}^\kappa \right) \Big|_{r=0} \\
 &= \ddot{\sigma} \left(x_{t+1}^\top (\boldsymbol{\theta}_i) \right) \left(\boldsymbol{\xi}_t^\top (\boldsymbol{\theta}_i) + x_{t+1}^\top \mathbf{w}_i \right) (\eta_{t+1})_{j,k} \\
 &\quad + \dot{\sigma} \left(x_{t+1}^\top (\boldsymbol{\theta}_i) \right) \left((\mathcal{R}_t)_{w,V}^\top (\boldsymbol{\theta}) + (\mathbf{u}_t)_{k,j}^\top \mathbf{w}_i + (\boldsymbol{\xi}_t)_j \delta_{k,i}^\kappa \right) \\
 \frac{\partial V_i(S_t)}{\partial r} &= \dot{\sigma}(x_t^\top \boldsymbol{\theta}_i) (\boldsymbol{\xi}_{t-1}^\top \boldsymbol{\theta}_i + x_t^\top \mathbf{w}_i)
 \end{aligned}$$

Appendix B. Generative Question Networks

The above experiments rely on an expert defined network; however, GVF networks can be specified more generally. In this section, we suggest a set of simple GVF primitives, that can be selected from without requiring expert information. These primitives are like the basic functional forms specified for neural networks: the activation functions. They play a similar role, in that the choice of them is likely to have an impact on prediction performance, but they can be generally successful with some experimental validation and without carefully designing specialized activations for each problem. We show that by generating a random set of GVF primitives, we can still get reasonable performance in Compass World and still enables one-step gradient updates.

We suggest an initial list of GVF primitives below, for our experiments. For this first work, we avoid more complex primitives, avoiding both GVFs with optimal policies and compositional GVFs. Composition of primitives is one avenue, though, to generate more useful GVF questions. The **termination functions** include *myopic discounts* ($\gamma = 0$), *horizon discounts* ($\gamma \in (0, 1)$) and *termination discounts* (the discount is set to a constant everywhere, except for at an event, which consists of a transition $(\mathbf{o}, a, \mathbf{o}')$). The **cumulants** include *stimuli cumulants* (the cumulant is one of the observations) and *event cumulants* (the cumulant is set to 1 at an event which consists of a transition $(\mathbf{o}, a, \mathbf{o}')$). The **policies**

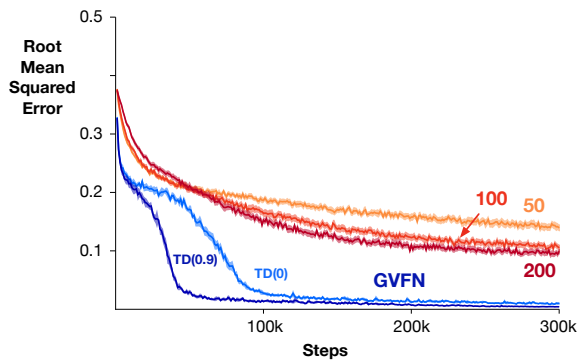


Figure 7: Compass world learning curves, for GVFNs defined in section B.

include *random policies* (an action is chosen at random) and *persistent policies* (follows a single action deterministically).

We generated random sets of GVF primitives for Compass World, of sizes 50, 100 and 200, with results in Figure 7. There is a significant gap in performance compared to the expert GVFN, which suggests more can be done to generate and select from these GVF primitives to obtain expressive GVFNs. In preliminary experiments, with re-generation and selection, we have found that we can significantly close this gap; however, we leave further investigation of generating GVF primitives to future work.

Constructing a GVFN from a set of primitive units shows potential and is the first step towards a principled method for discovering question networks online. One point of interest could be to employ a generate a test method where GVFs are removed based on their performance and average usefulness.